

Fundação  
para a Ciência  
e a Tecnologia

This work was financially supported by 2024.06584.CERN



# The ATLAS High-Granularity Timing Detector for the HL-LHC Project Status and Results

Helena Santos (LIP) on behalf of the ATLAS HGTD Collaboration

*14<sup>th</sup> International “Hiroshima” Symposium on the  
Development and Application of Semiconductor Tracking Detectors*

## HSTD 14

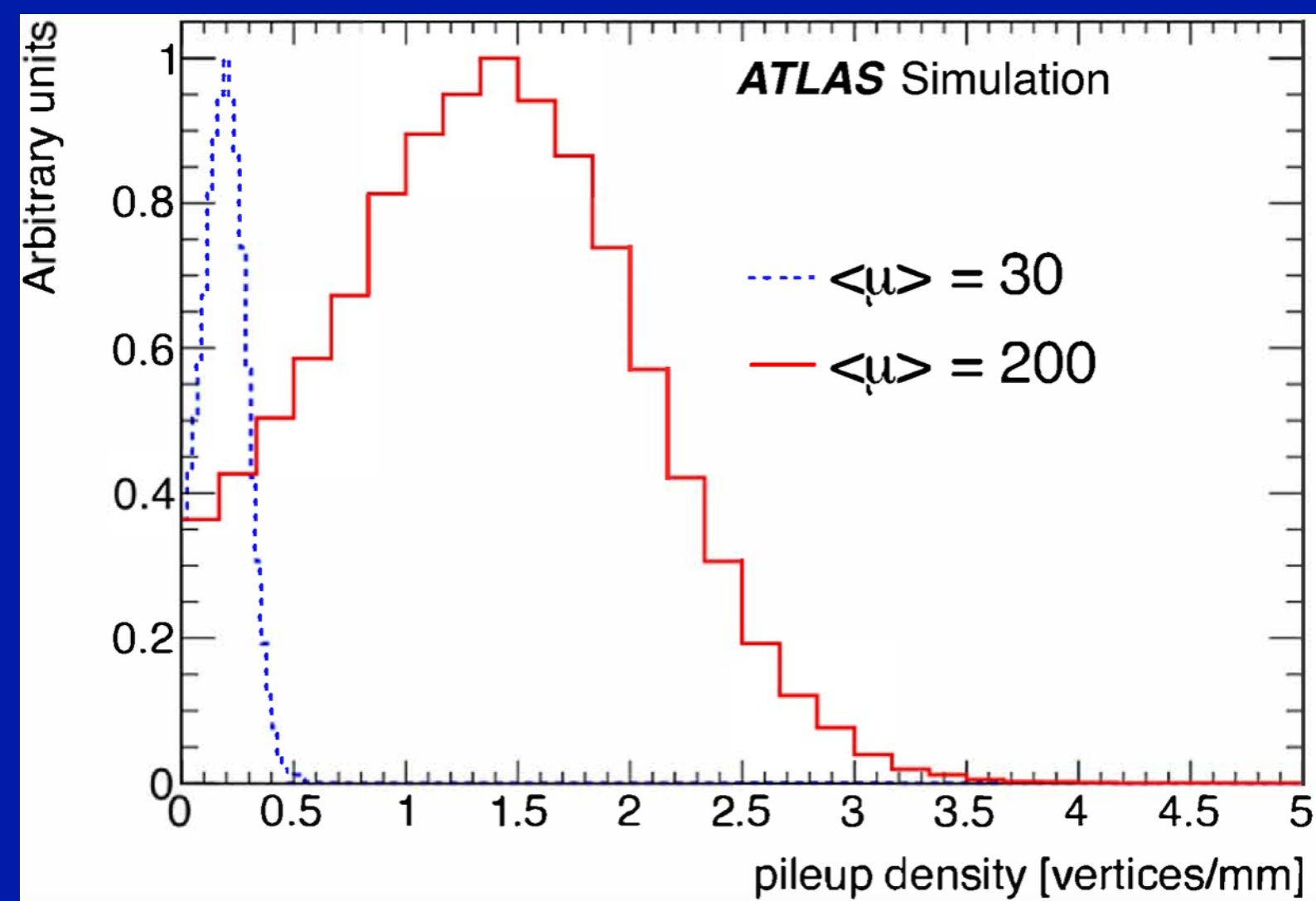
**November 16 - 21, 2025  
Academia Sinica, Taipei**

# Why do we need a timing detector in ATLAS

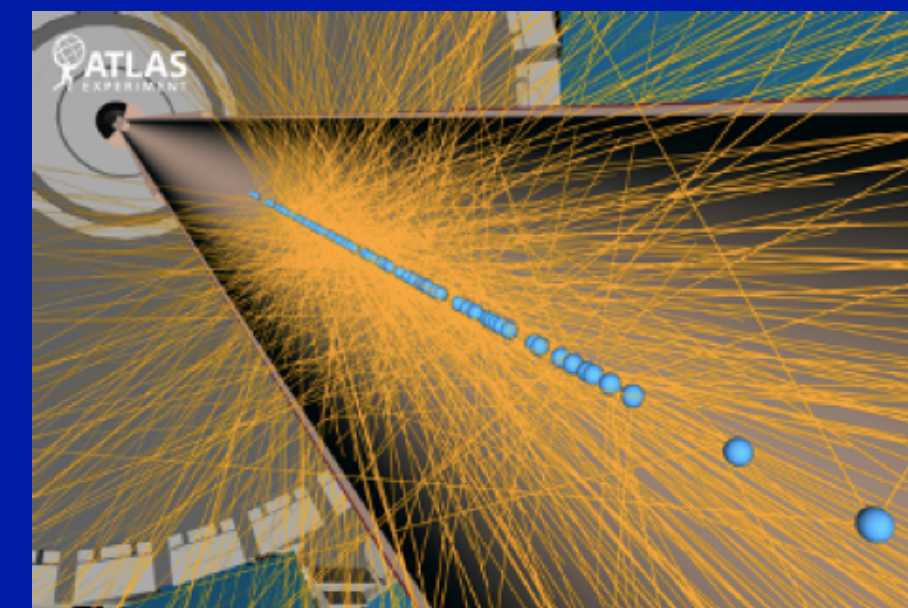
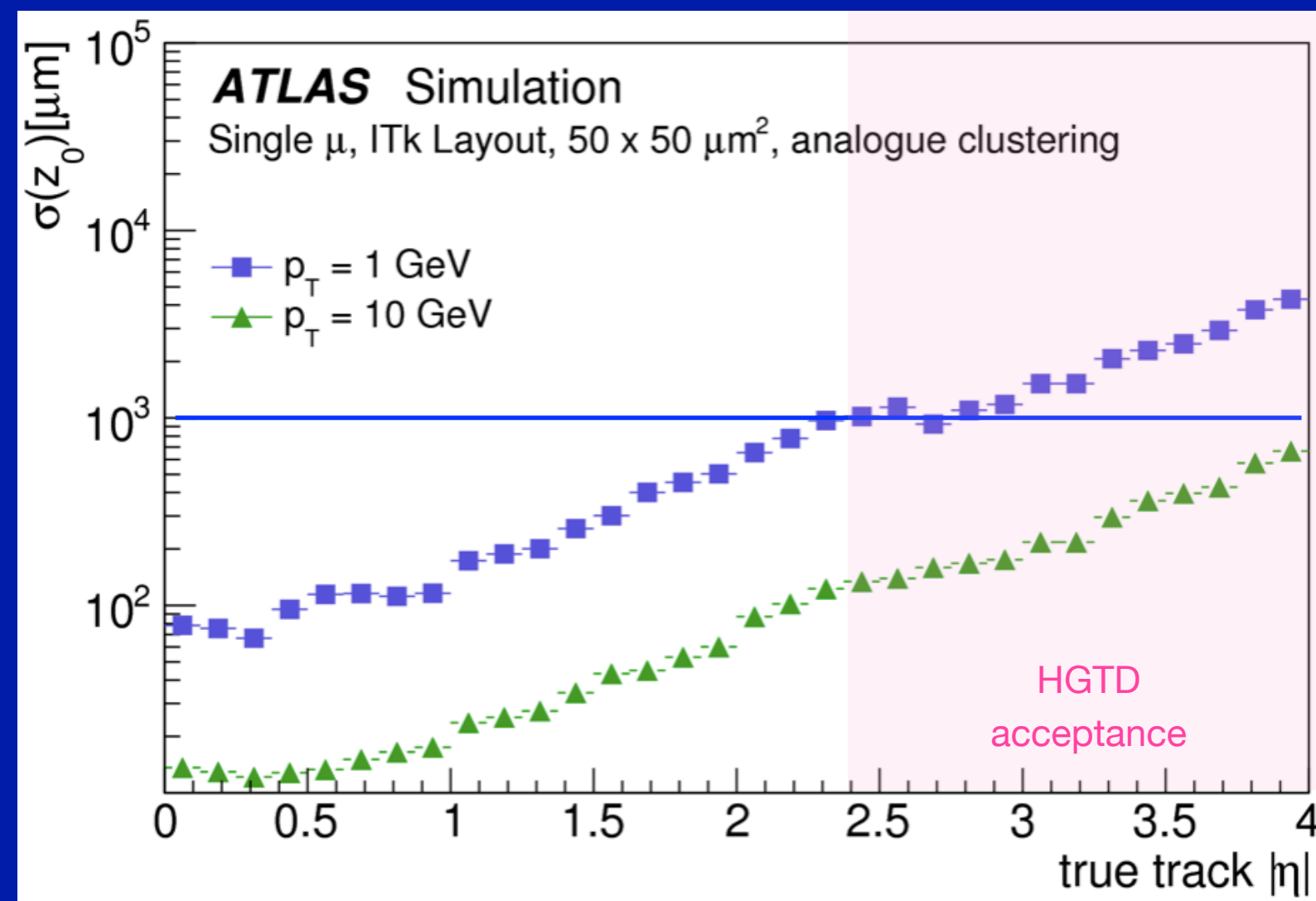
2

HGTD Public Results

Pileup  $\langle\mu\rangle$  can be 200 interactions per bunch-crossing at the HL-LHC. Vertex density will be on average 1.6 vertices/mm



Longitudinal impact-parameter track resolution,  $\sigma(z_0)$ , worsens at large  $\eta$



- Vertex spacing ( $\sim 0.6 \text{ mm}$ ) smaller than  $z_0$  resolution in the forward region
- Reconstructed vertices overlap
- Tracks from different vertices can be assigned to a given vertex

Ambiguity in track to vertex association

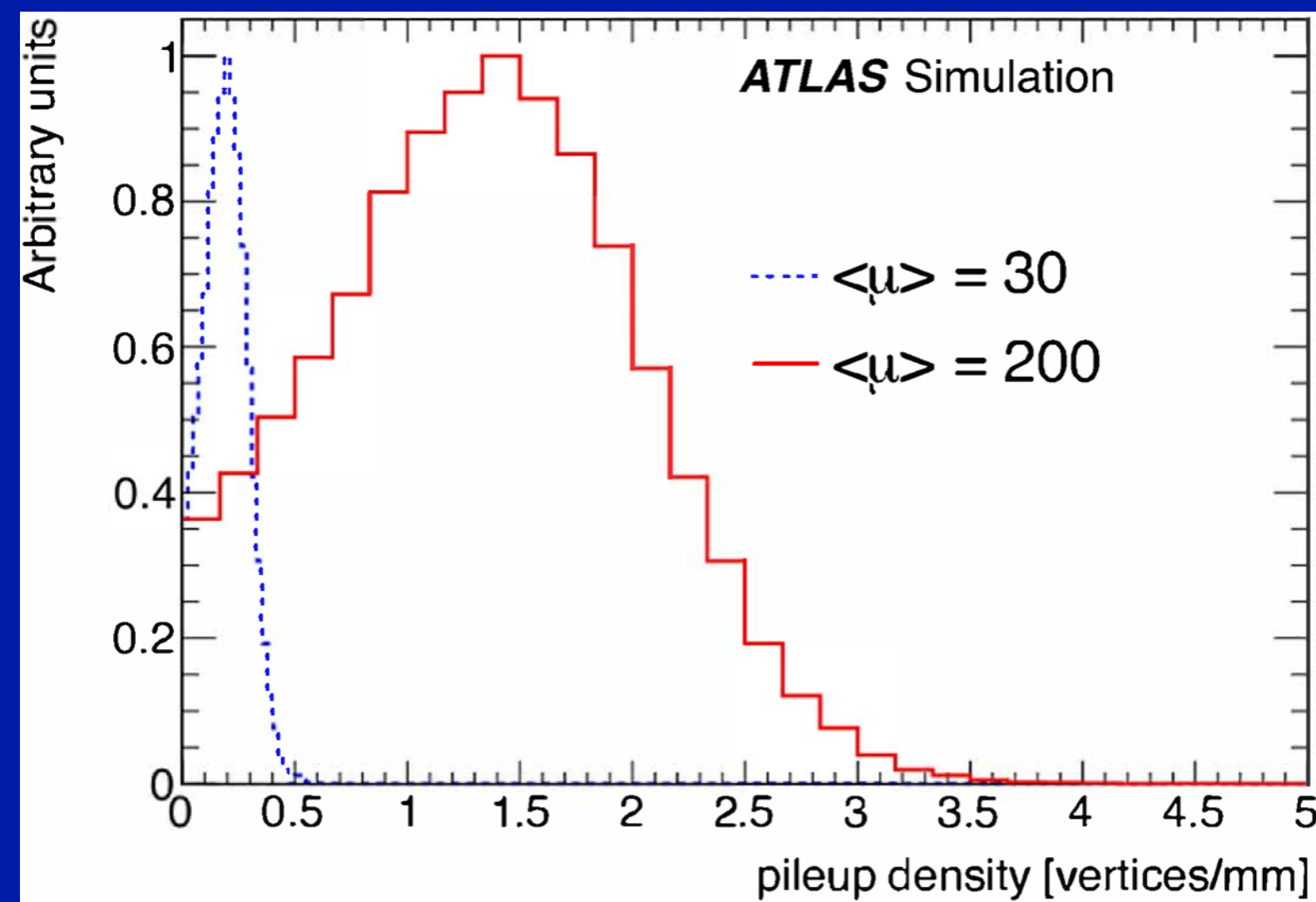


# Why do we need a timing detector in ATLAS

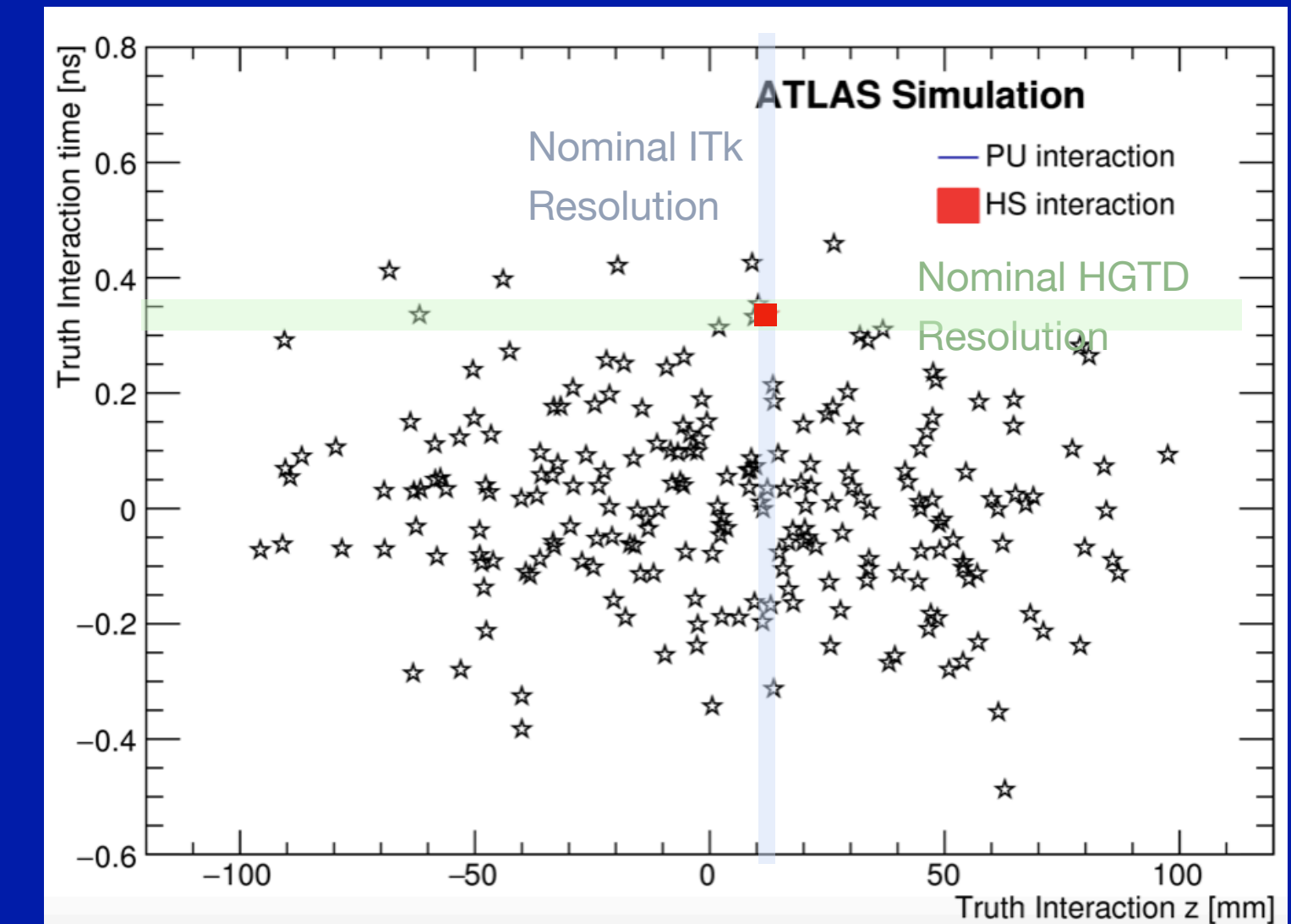
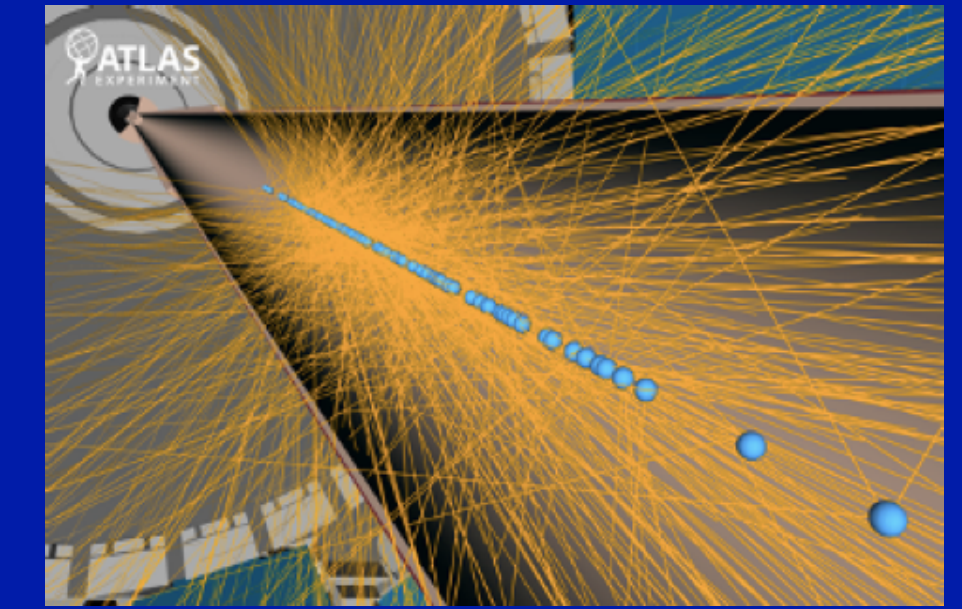
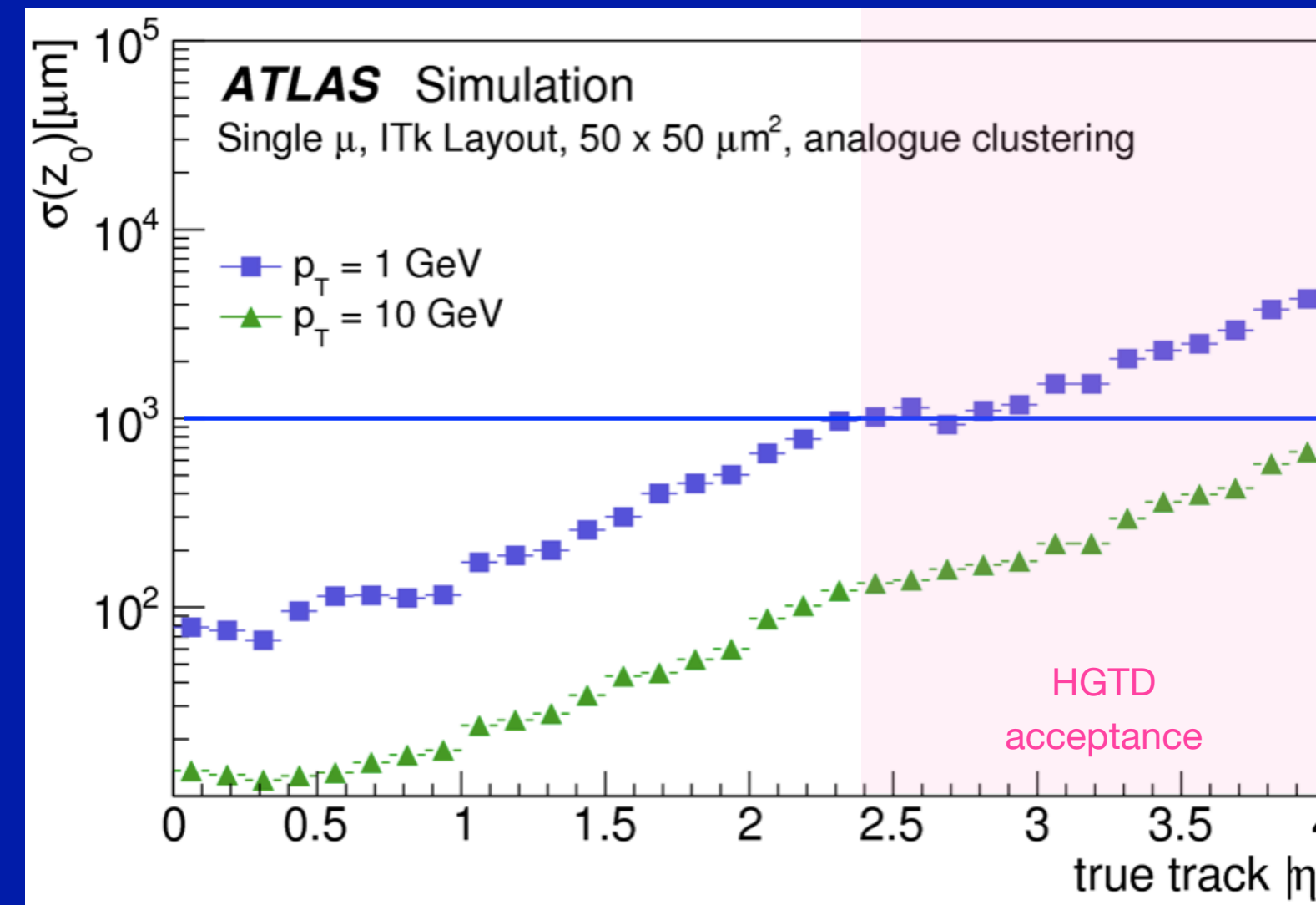
3

HGTD Public Results

Pileup  $\langle\mu\rangle$  can be 200 interactions per bunch-crossing at the HL-LHC. Vertex density will be on average 1.6 vertices/mm



Longitudinal impact-parameter track resolution,  $\sigma(z_0)$ , worsens at large  $\eta$



- Vertex spacing ( $\sim 0.6 \text{ mm}$ ) smaller than  $z_0$  resolution in the forward region
- Reconstructed vertices overlap
- Tracks from different vertices can be assigned to a given vertex

Ambiguity in track to vertex association

HGTD, with its precise timing, can associate a time to each track with unprecedented accuracy

It will work if  $\sigma_{\text{time}} \ll \text{vertex spread in time is } (\sim 180 \text{ ps})$



## Pad detector for precision timing in the forward region of ATLAS:

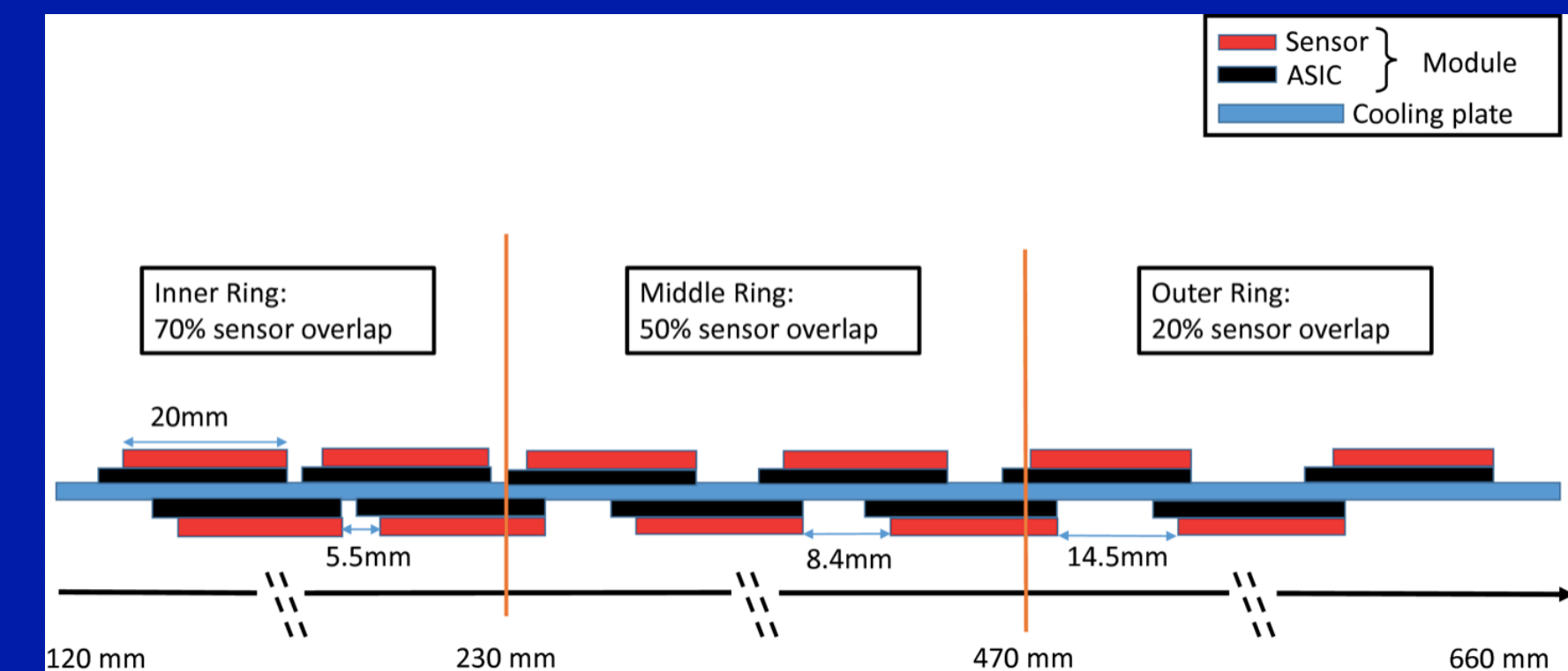
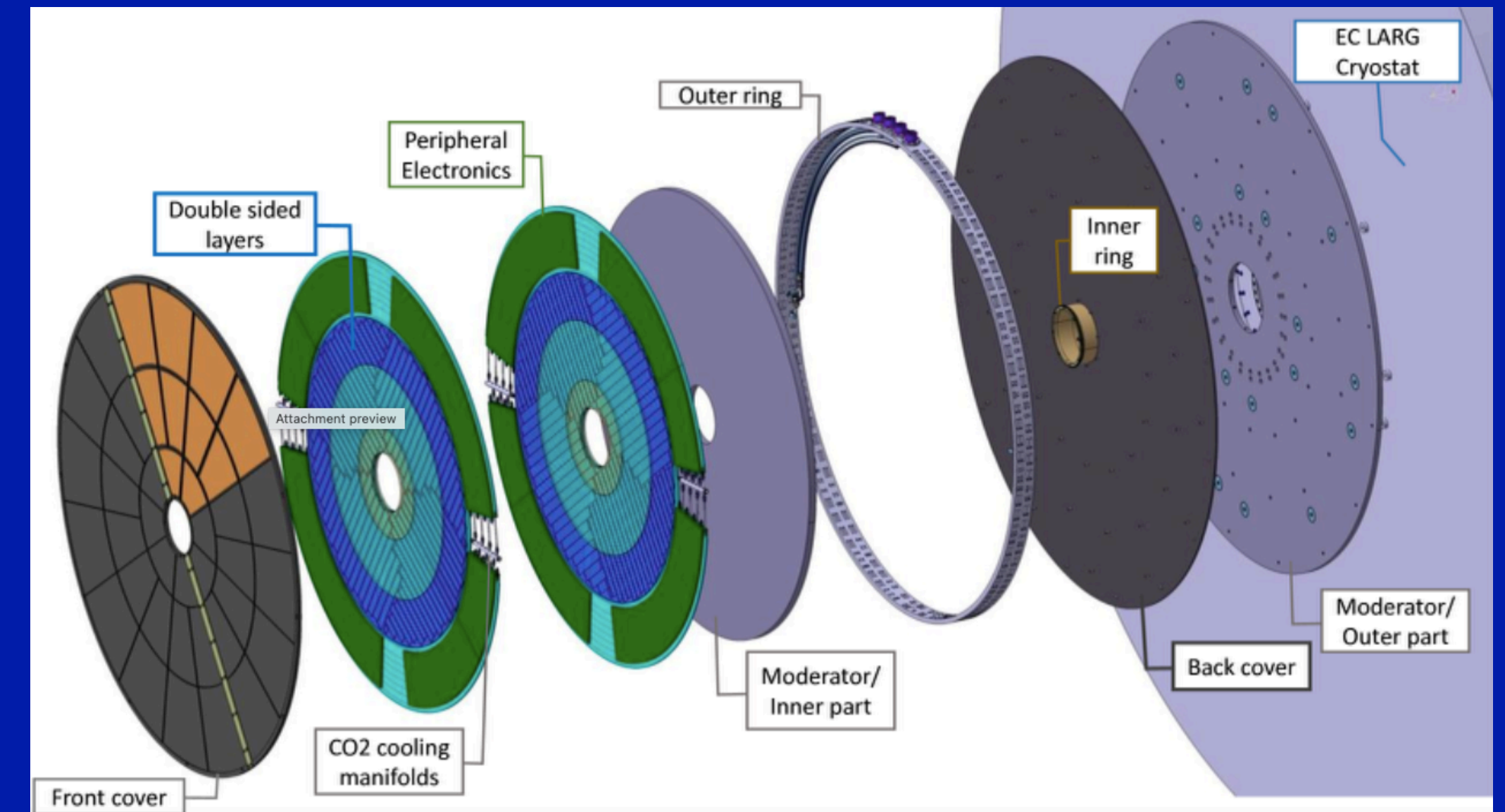
- Two endcaps positioned between the barrel and endcap calorimeters
- Each endcap: two disks with detectors mounted on both sides
- Located at  $\pm 3.5$  m from the interaction point
- Active coverage:  $2.4 < |\eta| < 4$
- Radial range:  $120 \text{ mm} < r < 640 \text{ mm}$
- Radiation hardness:
  - Up to  $2.5 \times 10^{15} \text{ n}_{\text{eq}}/\text{cm}^2$
  - 2 MGy total ionising dose (TID)

## Performance Goals

- Time resolution (per hit): 40–85 ps up to  $4000 \text{ fb}^{-1}$
- Time resolution (per track): 30–50 ps up to  $4000 \text{ fb}^{-1}$

## Luminosity Measurement

- Counts hits at 40 MHz, bunch-by-bunch
- Target precision: 1% luminosity uncertainty for HL-LHC





16064 silicon sensors with internal gain based on LGAD (Low Gain Avalanche Diode) technology

## Pad & Sensor specifications

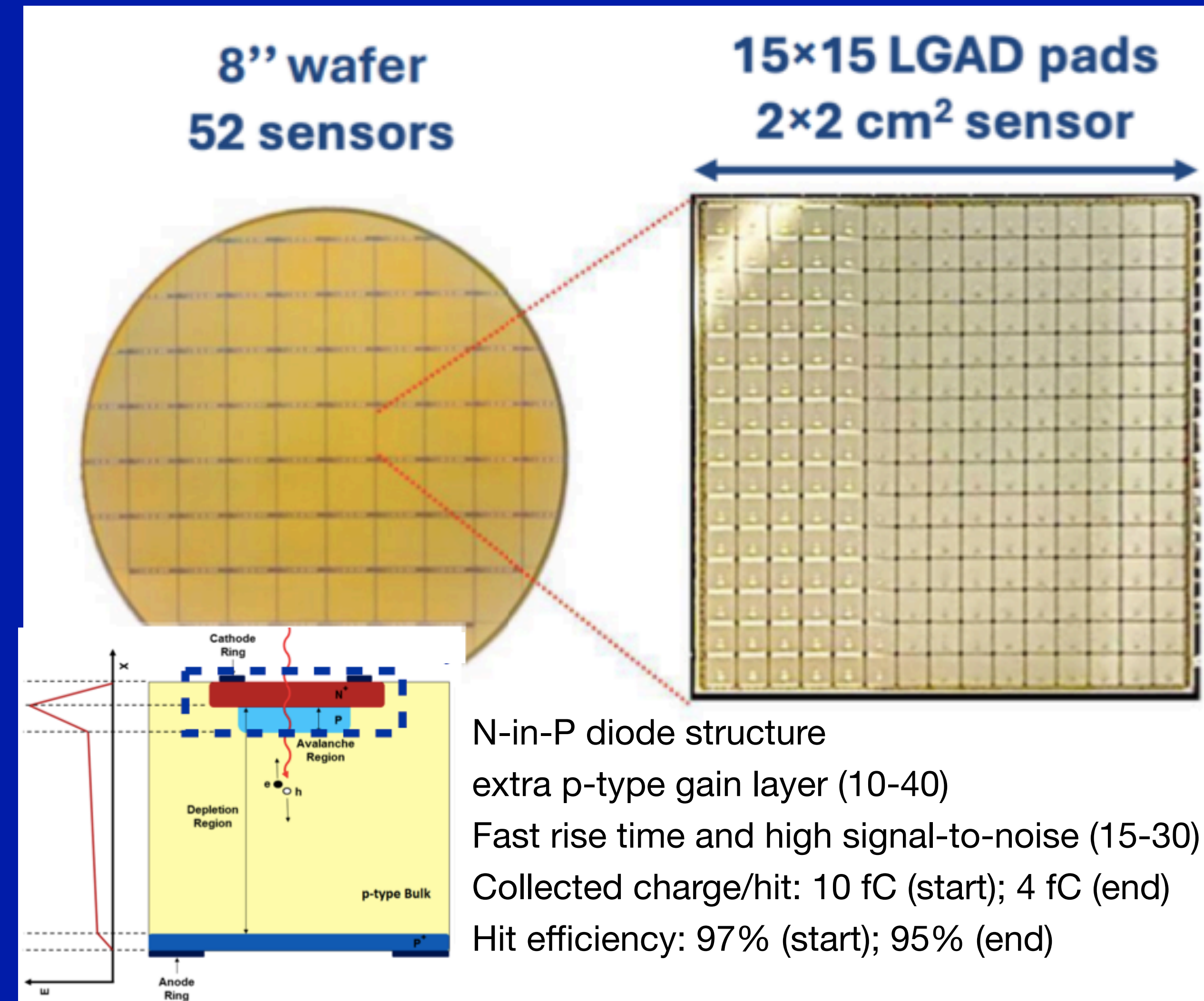
- Pad matrix:  $15 \times 15 = 225$  pad per sensor
- Pad size:  $1.3 \text{ mm} \times 1.3 \text{ mm}$
- Active thickness:  $50 \text{ }\mu\text{m}$
- Total thickness:  $775 \text{ }\mu\text{m}$

## Detector design

- Four sensor layers  $\rightarrow$  ensures  $\geq 2$  hits per track

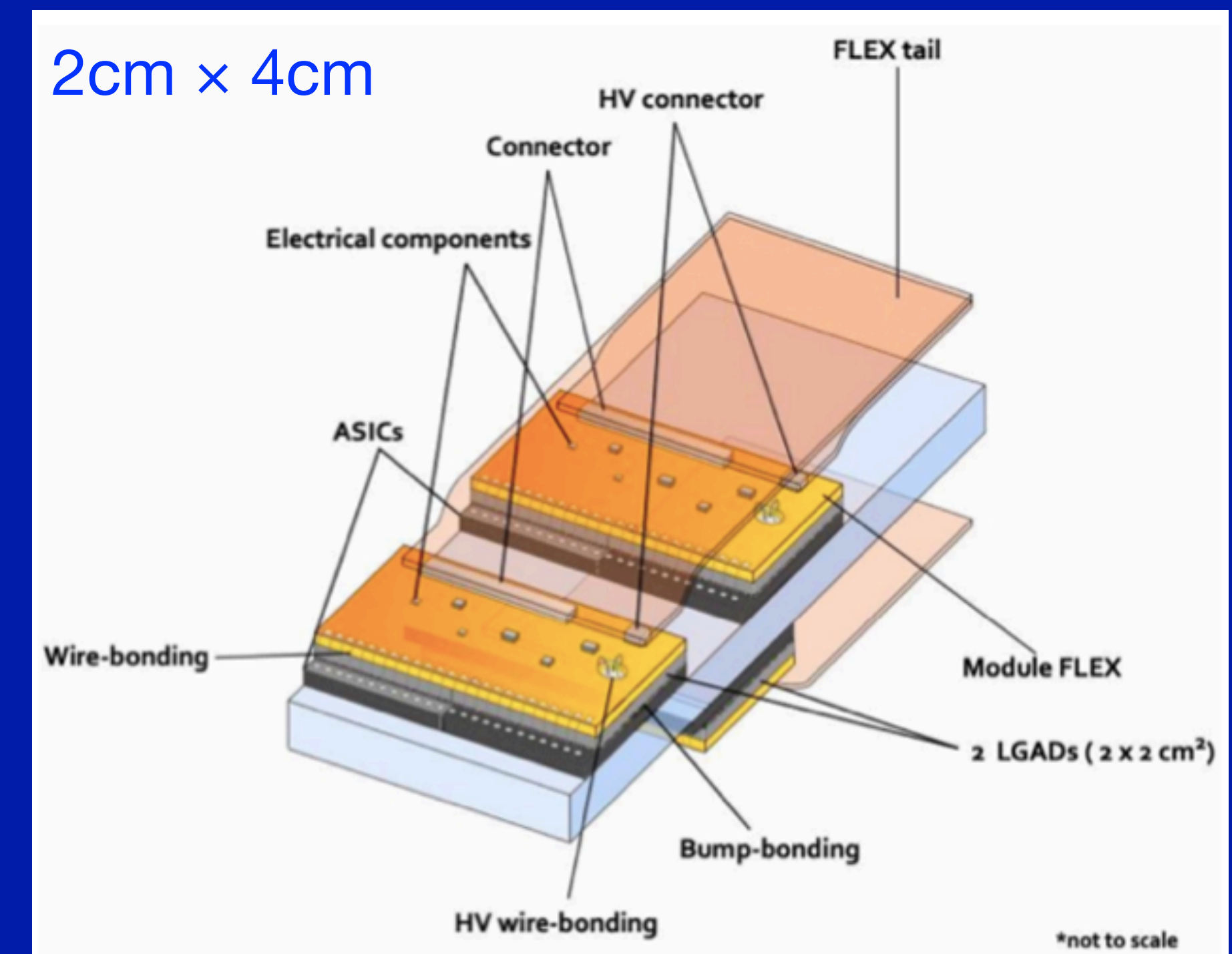
## Sensor production

- 8-inch silicon wafers
- 52 sensor arrays per wafer



## ATLAS LGAD Timing Integrated ReadOut Chip

- Two readout ASICs bump-bonded to two LGAD sensors, mounted on a PCB for power and communication
- A FLEX tail carrying HV, LV and signals to/from peripheral electronics boards (PEB)
- Per-module HV settings to accommodate the variation of radial fluence
- LGAD sensor temperature will be maintained at  $-30\text{ }^{\circ}\text{C}$  using an evaporative  $\text{CO}_2$  cooling manifold integrated in the disks



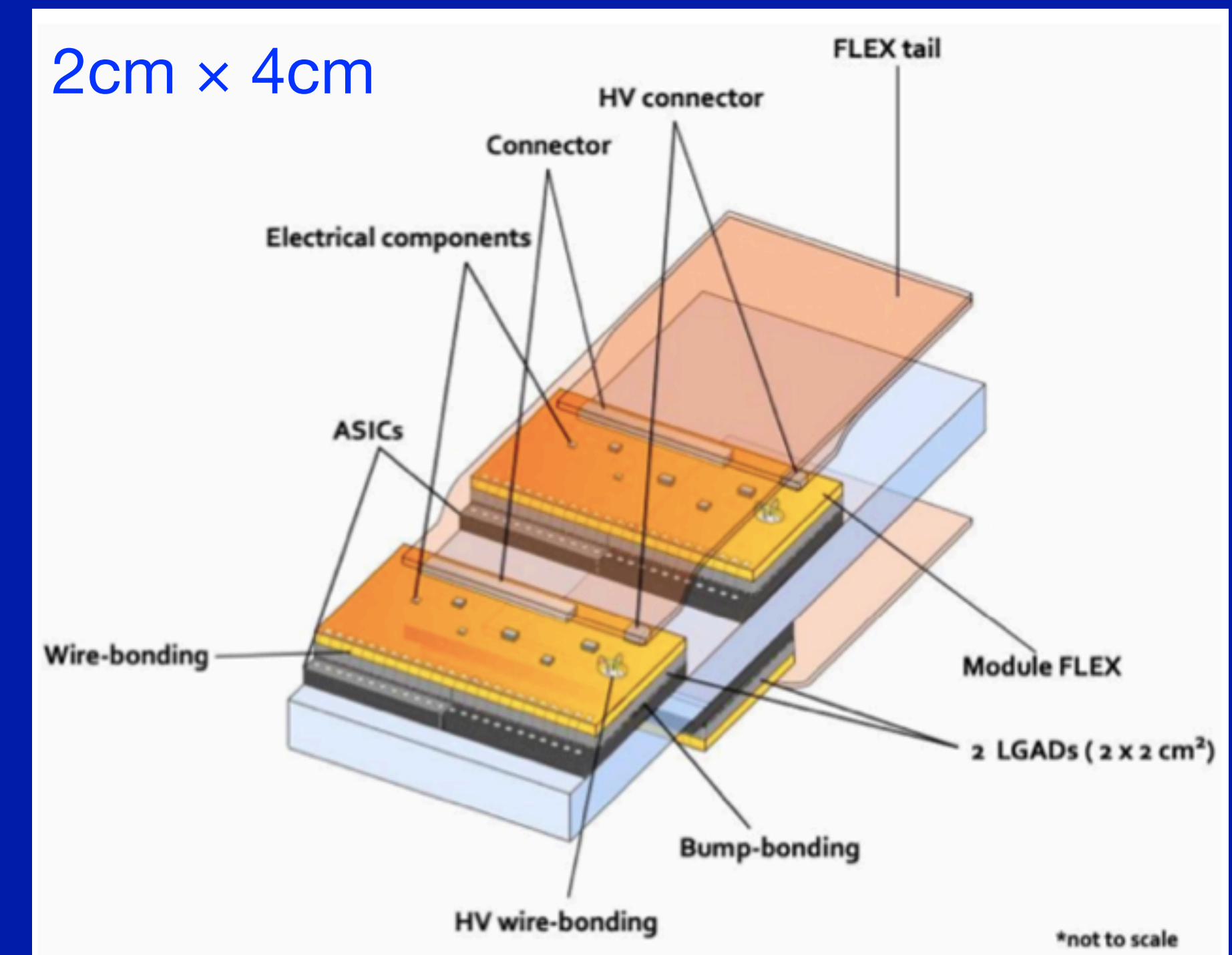


## ATLAS LGAD Timing Integrated ReadOut Chip

- Two readout ASICs bump-bonded to two LGAD sensors, mounted on a PCB for power and communication
- A FLEX tail carrying HV, LV and signals to/from peripheral electronics boards (PEB)
- Per-module HV settings to accommodate the variation of radial fluence
- LGAD sensor temperature will be maintained at  $-30\text{ }^{\circ}\text{C}$  using an evaporative  $\text{CO}_2$  cooling manifold integrated in the disks

### Specifications:

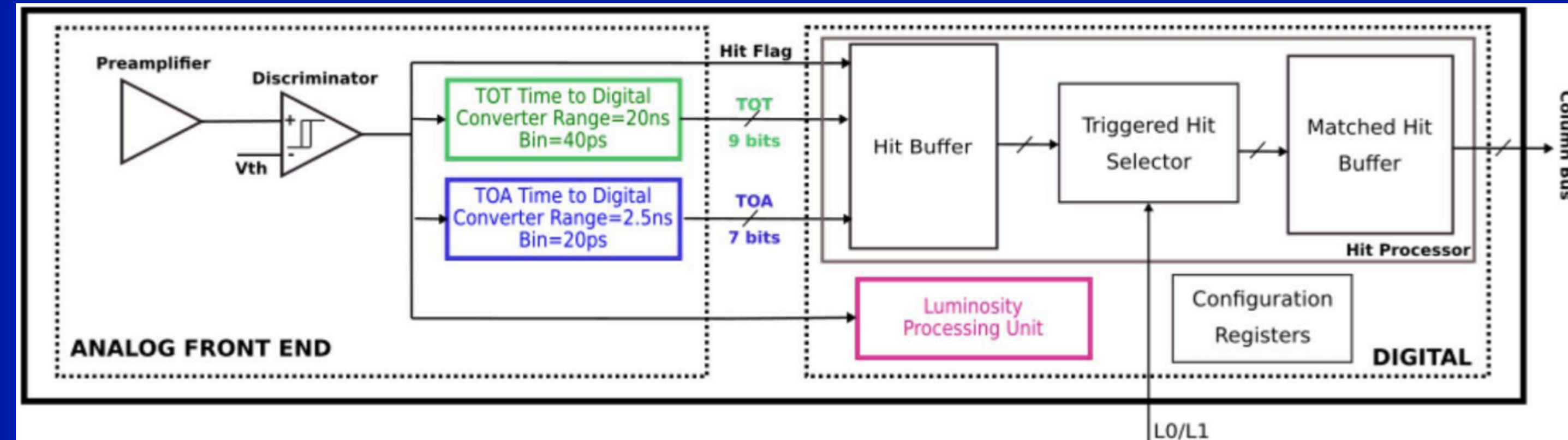
- Rad-Tolerant 130 nm CMOS (TSMC)
- 225 (15x15) channels, matching the sensor number
- Measures the Time Of Arrival (TOA) and Time Over Threshold (TOT, for time-walk correction)
- Minimum discriminator threshold: 2 fC
- Timing resolution: Jitter  $< 25\text{ ps}$  @ 10 fC and  $< 65\text{ ps}$  @ 4 fC
- Cooling power requirement (20 kW/vessel):  
Overall (sensor) power density:  $< 300\text{ mW/cm}^2$  ( $100\text{ mW/cm}^2$ )





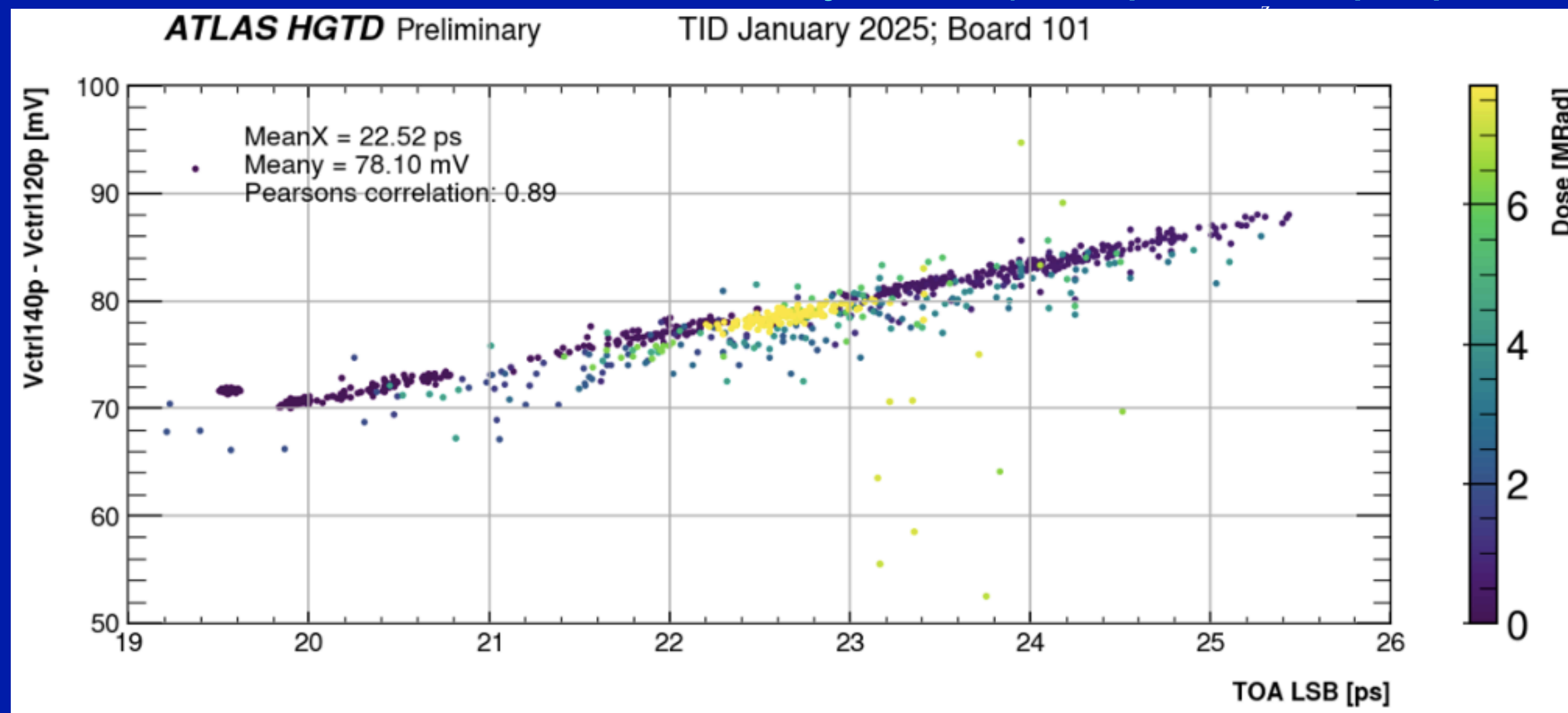
## HGTD Public Results

- Timing and hit data stored in local registers
- On Level0 Accept they are sent off-chip ( $\leq 35 \mu\text{s}$  latency)
- Luminosity derived from hit rate per ASIC per bunch-crossing

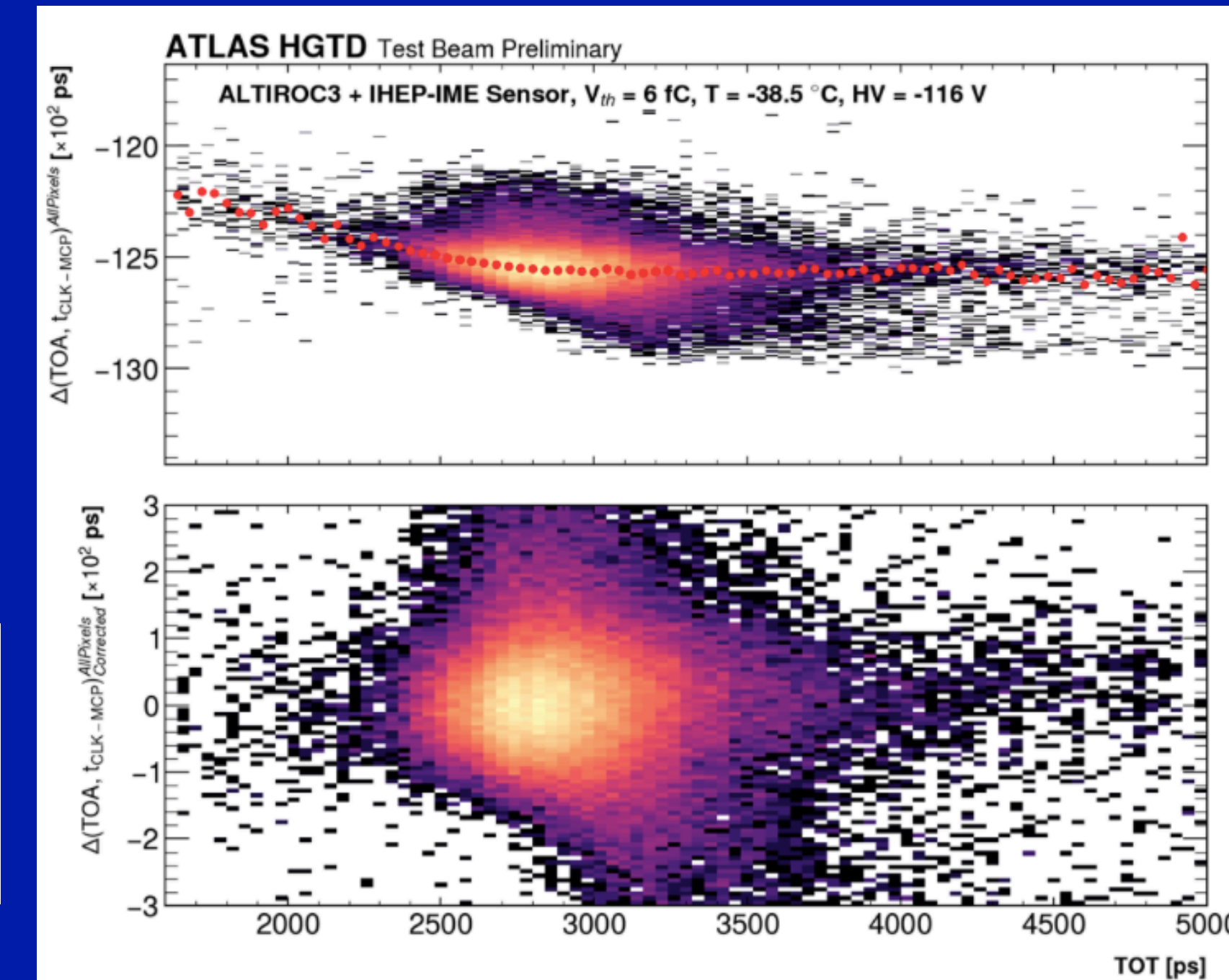
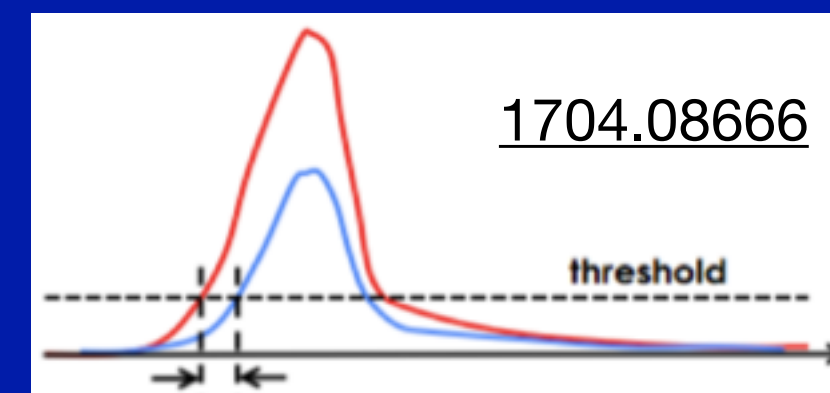


TOA before and after TOT-based time-walk correction

TOA TDC calibration: Vernier delay lines (120 ps / 140 ps per stage)



TOT: used to correct TOA shifts due to time-walk



Larger  $V_{\text{ctrl}}$  difference  $\rightarrow$  wider time bin  
Stable correlation under irradiation

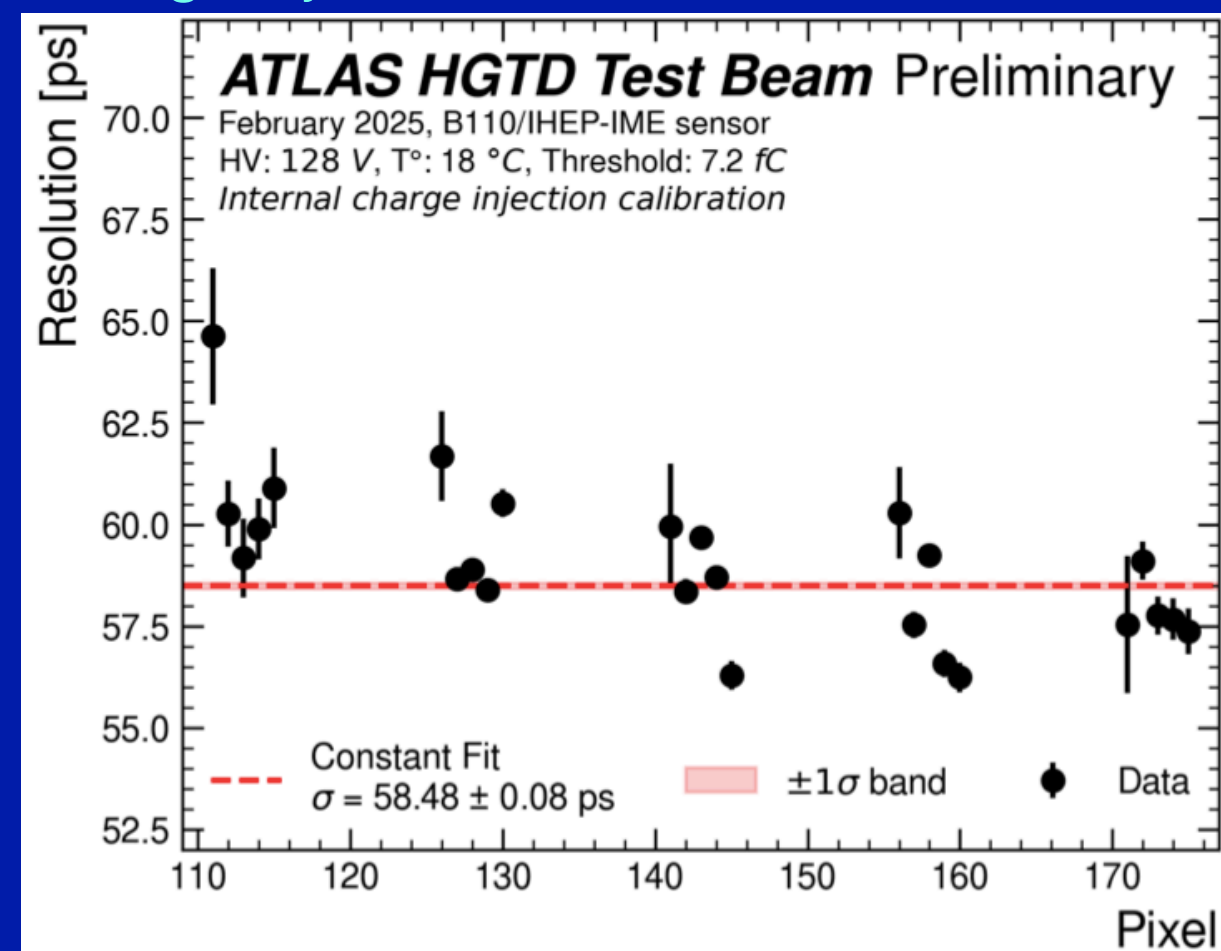
TOA residuals are flat



$$\sigma_{total}^2 = \underbrace{\sigma_{Landau}^2 + \sigma_{jitter}^2}_{sensor} + \underbrace{\sigma_{TDC}^2 + \sigma_{clock}^2 + \sigma_{time-walk}^2}_{ASIC + readout}$$

- TOA calibration applied here includes:
  - Per-channel TOA linearization, performed using either internal charge injection (ASIC) or testbeam data (with LGAD signals)
  - TOT-based time-walk correction, derived from testbeam TOT–TOA curves

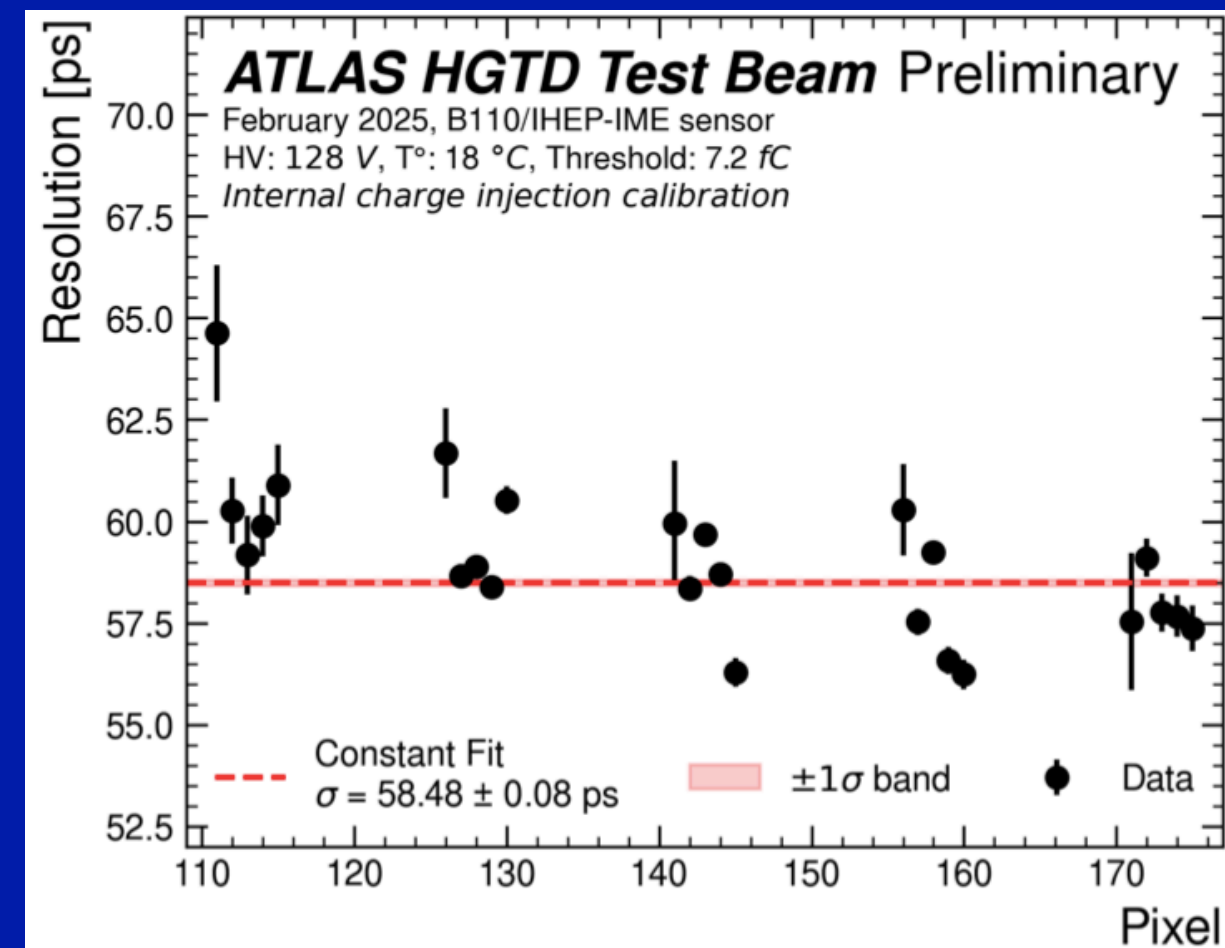
Charge injection, no TWC



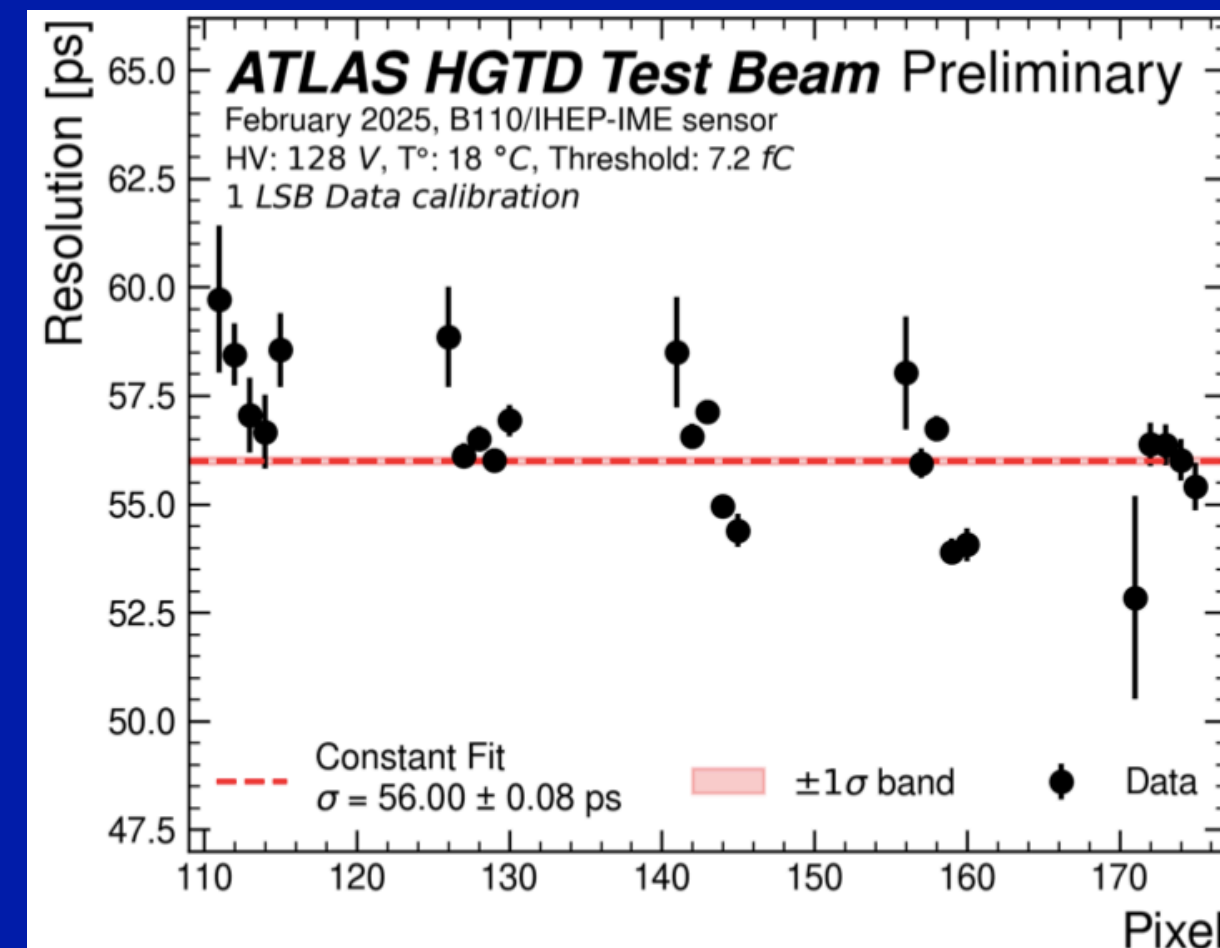
$$\sigma_{total}^2 = \overbrace{\sigma_{Landau}^2 + \sigma_{jitter}^2}^{sensor} + \overbrace{\sigma_{TDC}^2 + \sigma_{clock}^2 + \sigma_{time-walk}^2}^{ASIC + readout}$$

- TOA calibration applied here includes:
  - Per-channel TOA linearization, performed using either internal charge injection (ASIC) or testbeam data (with LGAD signals)
  - TOT-based time-walk correction, derived from testbeam TOT–TOA curves

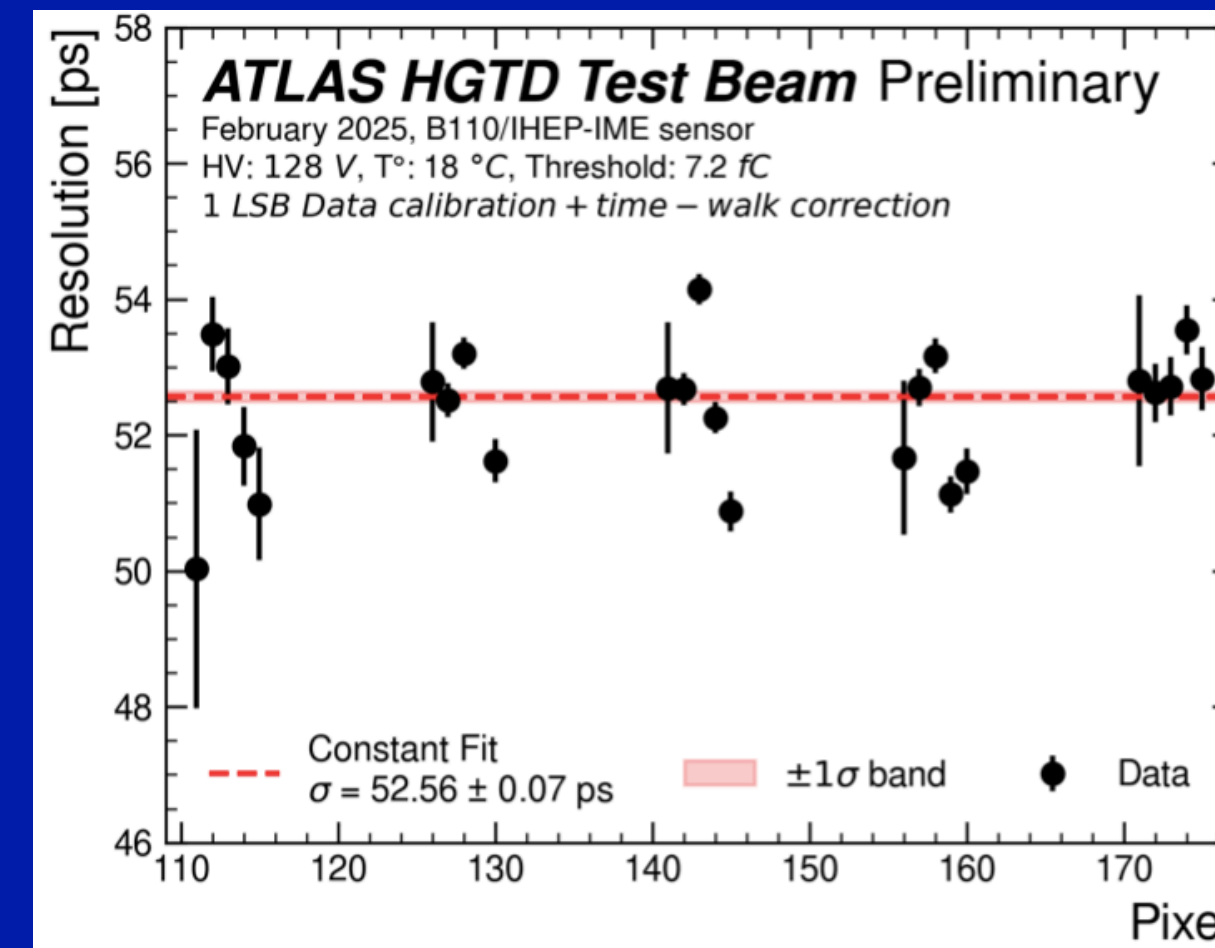
Charge injection, no TWC



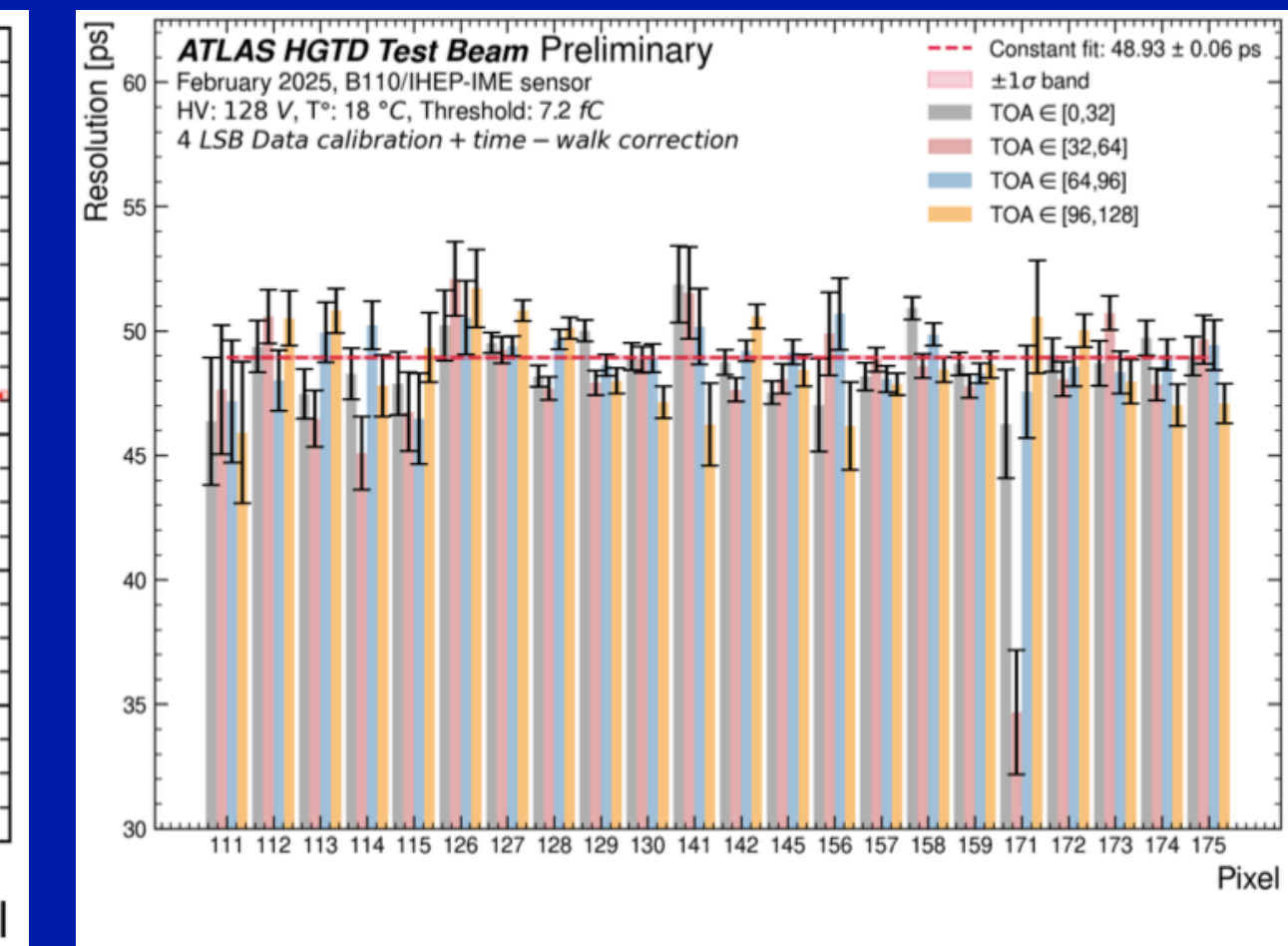
TB data, no TWC



TB data, with TWC



TB data, 4 LSB corr. for DNL, with TWC



In testbeam data, time resolution is extracted from residuals between calibrated TOA (ASIC) and MCP-PMT reference

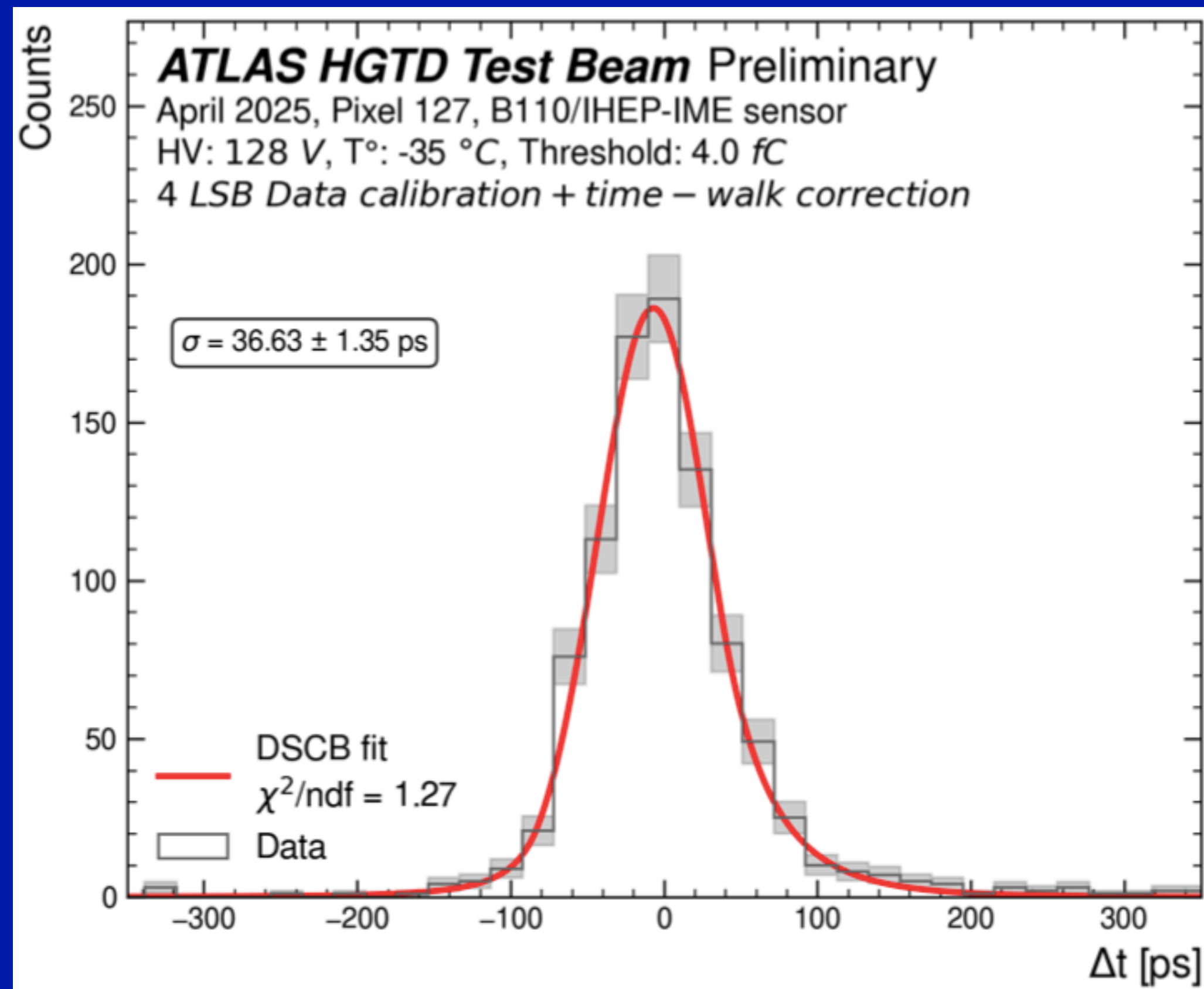
Data-driven method improves resolution significantly, exposing the intrinsic sensor limit



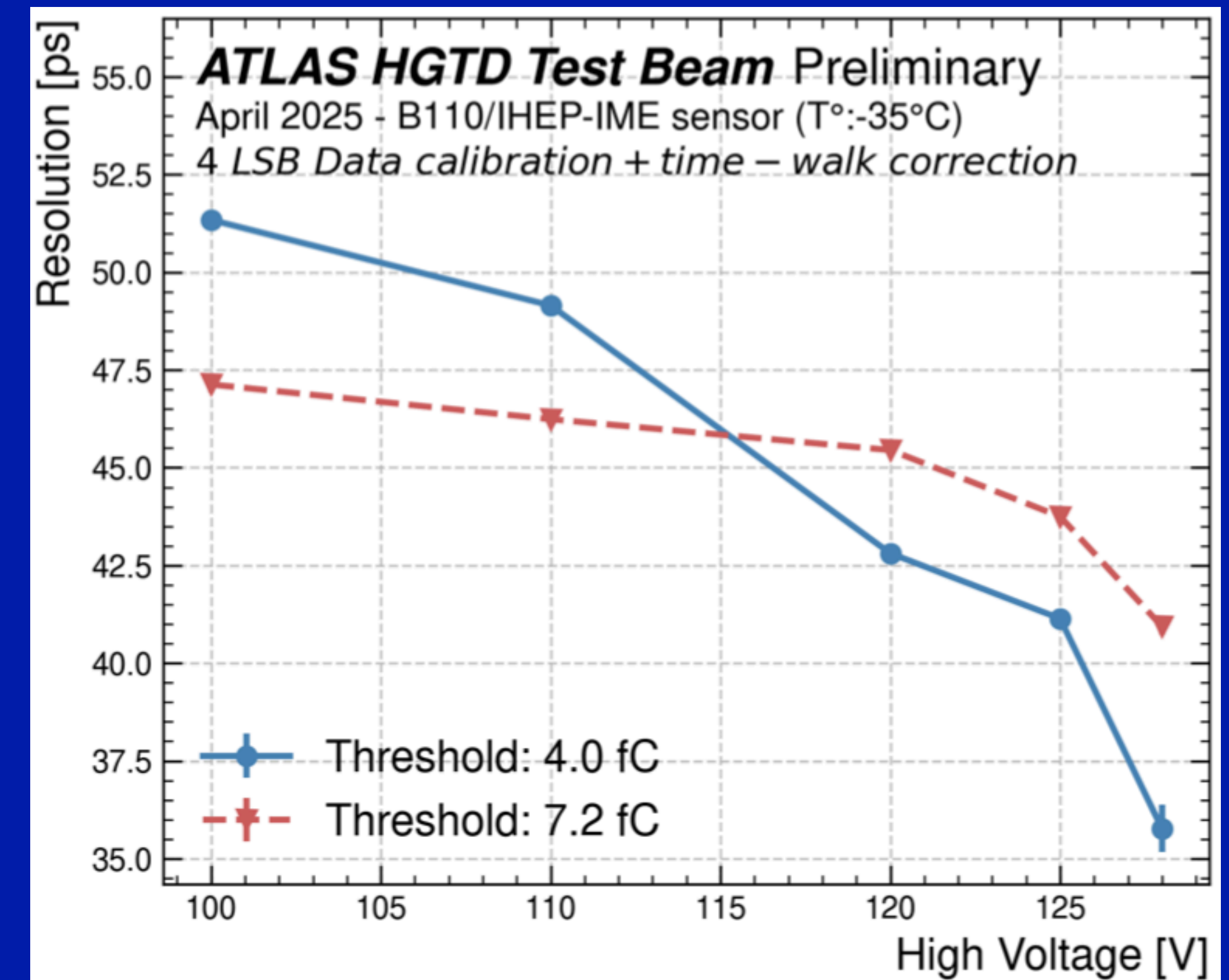
$$\sigma_{total}^2 = \overbrace{\sigma_{Landau}^2 + \sigma_{jitter}^2}^{sensor} + \overbrace{\sigma_{TDC}^2 + \sigma_{clock}^2 + \sigma_{time-walk}^2}^{ASIC + readout}$$

Performance of ALTIROC3 in optimal operating conditions:

- Low temperature (−35 °C), high bias (>120 V), low threshold (4 fC)



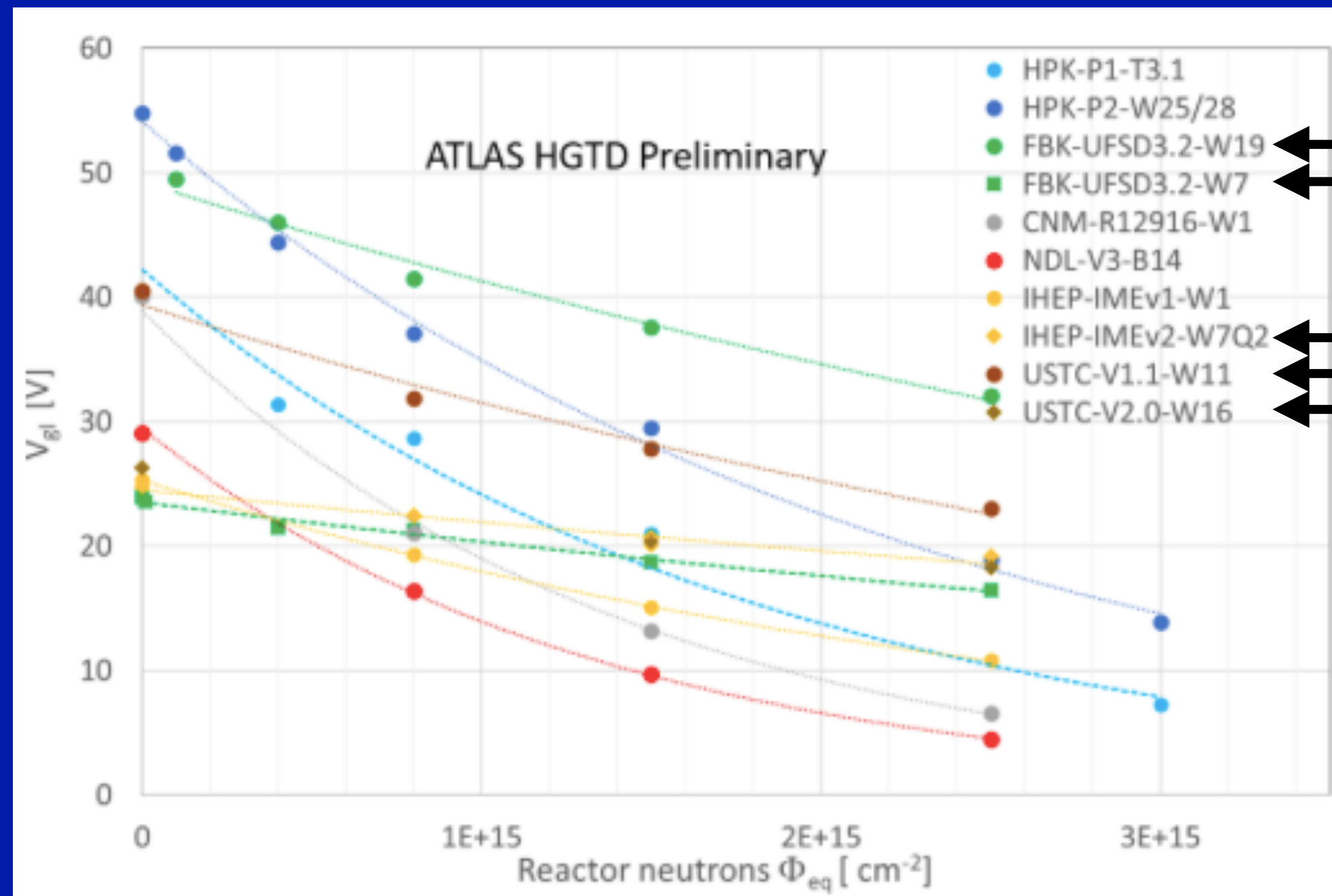
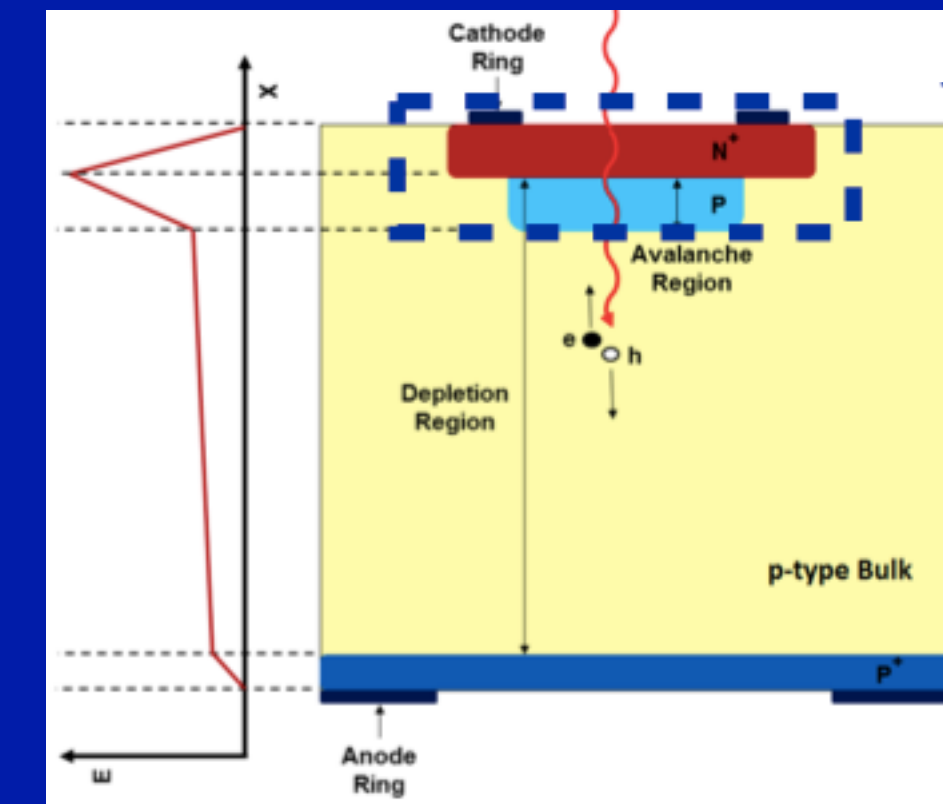
$$\Delta t = \text{TOA} \times \text{LSB} - (t_{\text{Clock}} - t_{\text{MCP}})$$



Timing resolution reaches 36 ps

Radiation induces acceptor removal in the p<sup>+</sup> gain layer, reducing the electric field and leading to loss of gain

→ Study gain layer depletion voltage,  $V_{gl}$ , dependence on fluence:  $V_{gl} = V_{gl,0} \times e^{-C\Phi_{eq}}$



From C-V measurements: lowest acceptor removal with carbon-enriched wafers



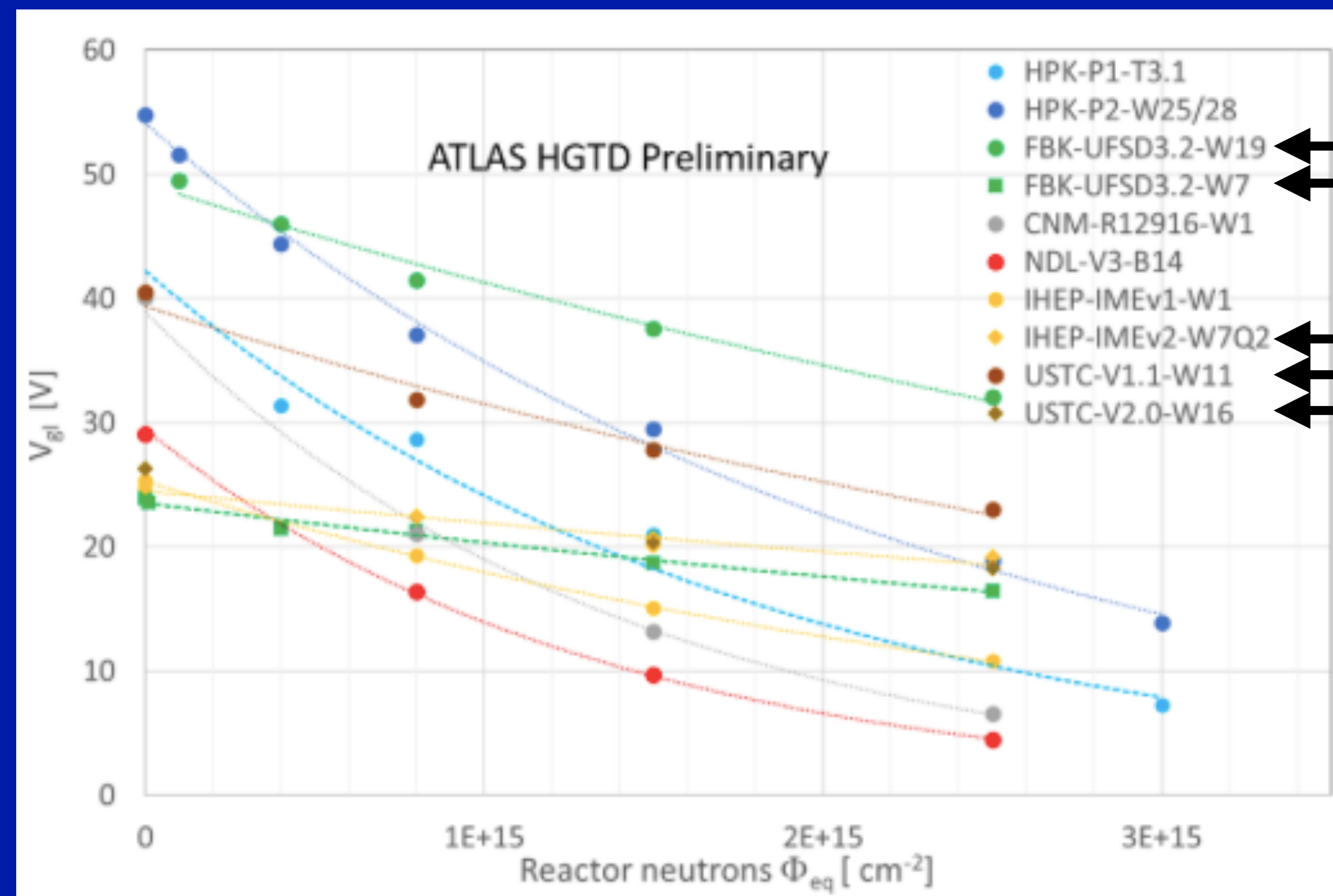
Radiation induces acceptor removal in the  $p^+$  gain layer, reducing the electric field and leading to loss of gain

→ Study gain layer depletion voltage,  $V_{gl}$ , dependence on fluence:  $V_{gl} = V_{gl,0} \times e^{-C\Phi_{eq}}$

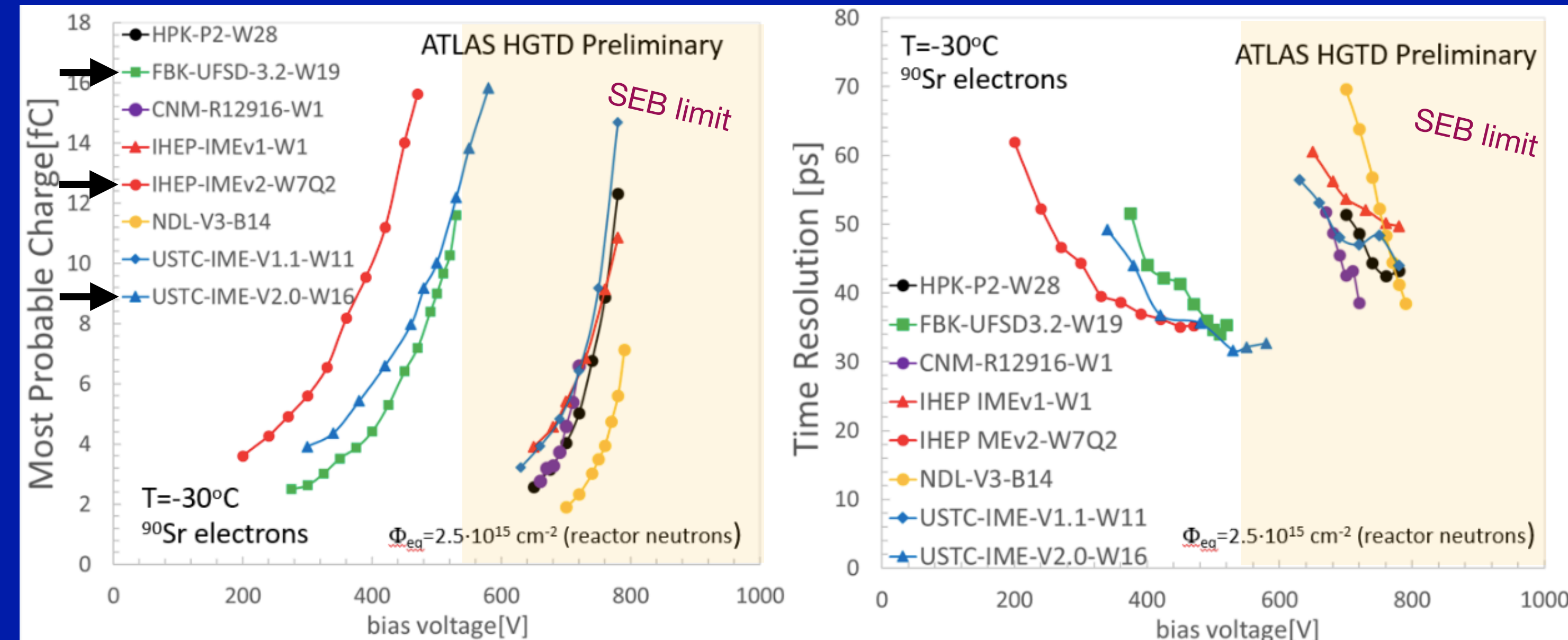
Recover by increasing the bias

- Limit imposed by Single Event Burnout (SEB) effect (local breakdown of electric field)

→  $V_{max} \sim 550$  V for  $50 \mu m$  thickness



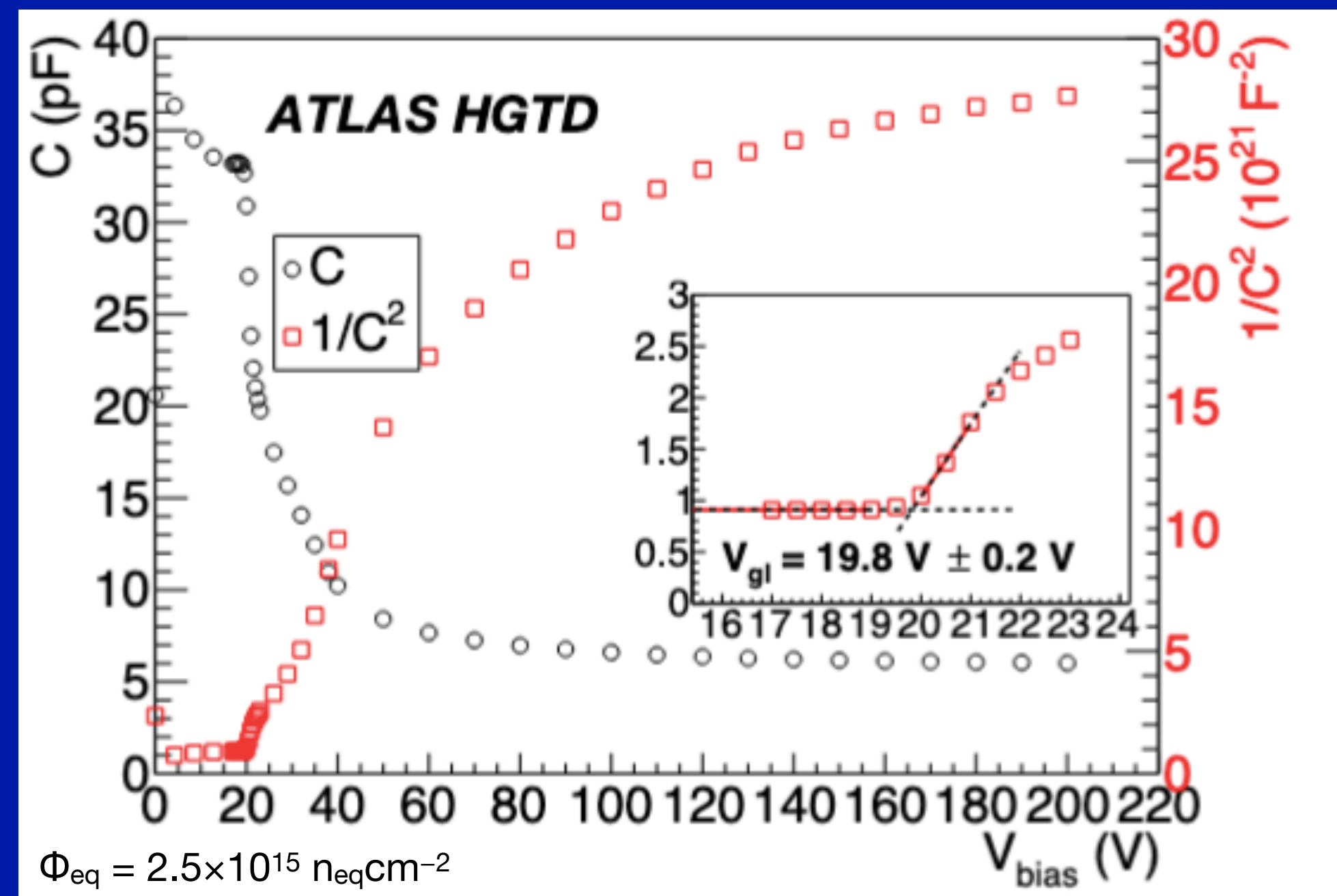
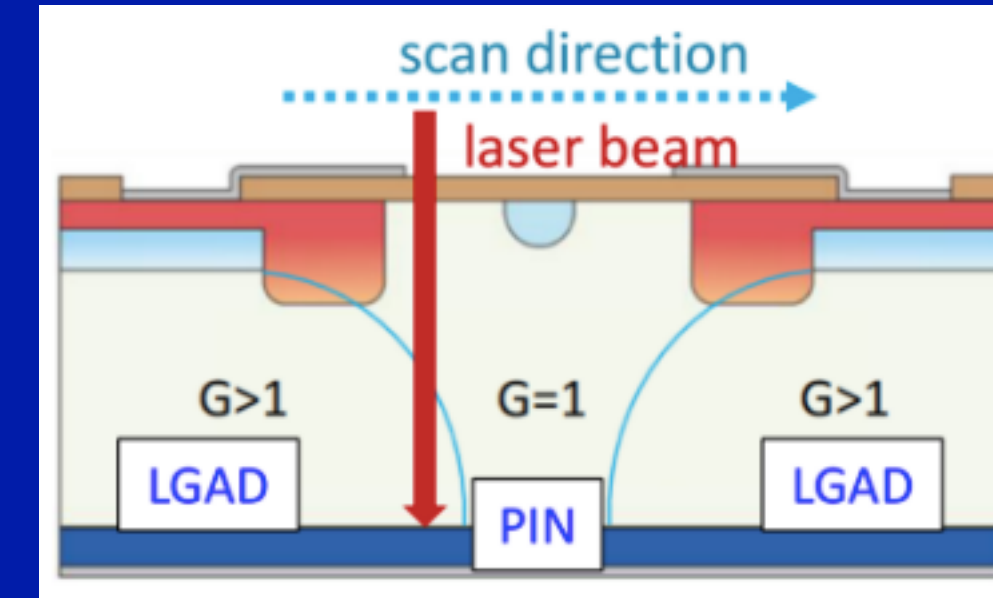
From C-V measurements: lowest acceptor removal with carbon-enriched wafers



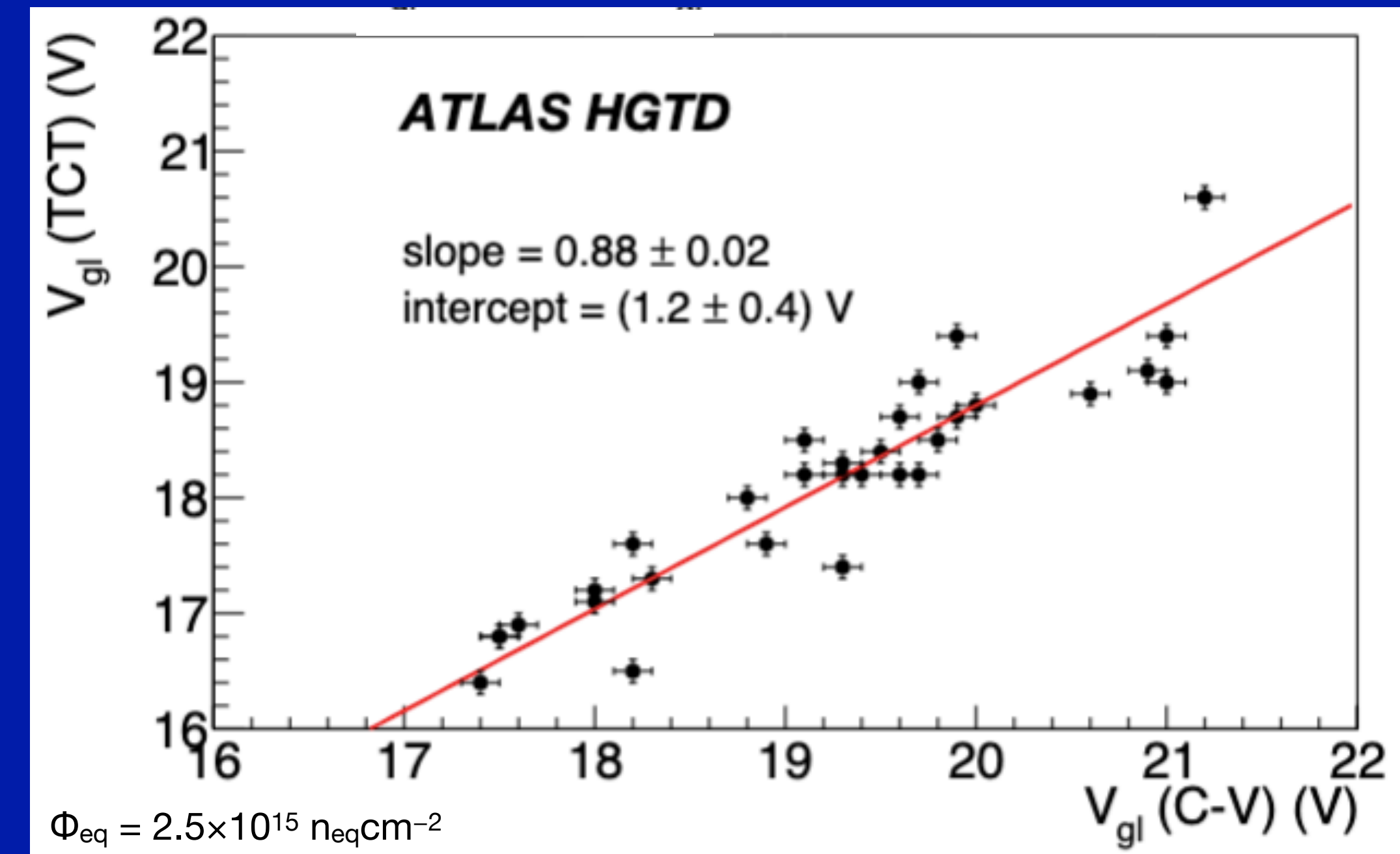
FBK-UFSC-2.3-W19, IHEP-IMEv2-W7Q2, USTC-IME-V2.0-W16 sensors show stable performance at much lower bias voltages than non-carbon enriched wafers

Transition Current Technique - performed in the interface region of two LGAD devices

- $V_{gl}$  extraction
- Gain dependence on bias voltage
- Sensor leakage current
- Effective interpad distance



Inset shows  $V_{gl}$  extraction from the intersection of linear fits

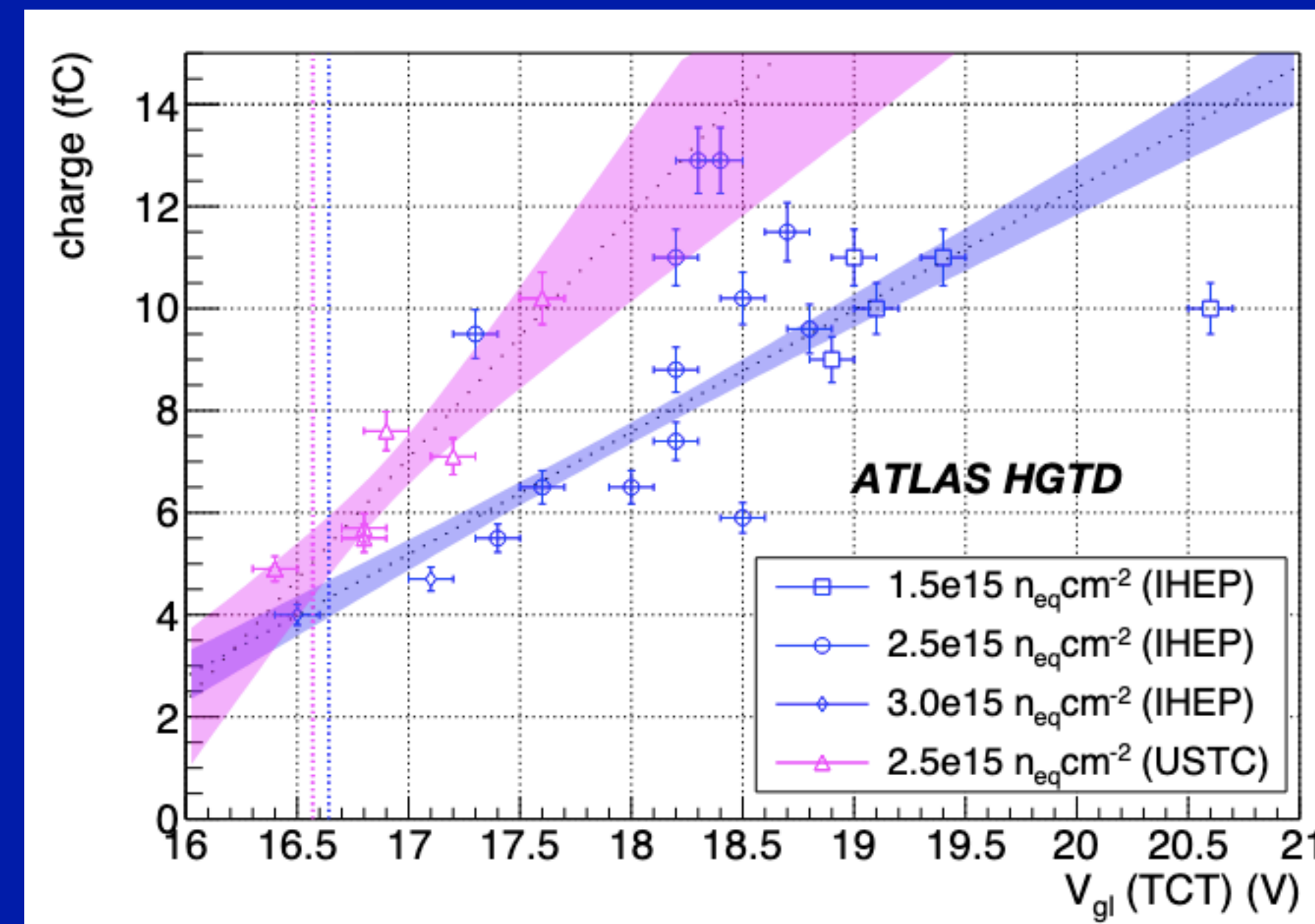


Systematic offset between  $V_{gl}$  from TCT and C-V measurements  
→ Charge-collection vs AC electrical responses



Correlation between most probable collected charge from  $^{90}\text{Sr}$  MIP and  $V_{gl}$  for two sensor designs: IHEP and USTC, both from IME

[arXiv:2509.09187](https://arxiv.org/abs/2509.09187)



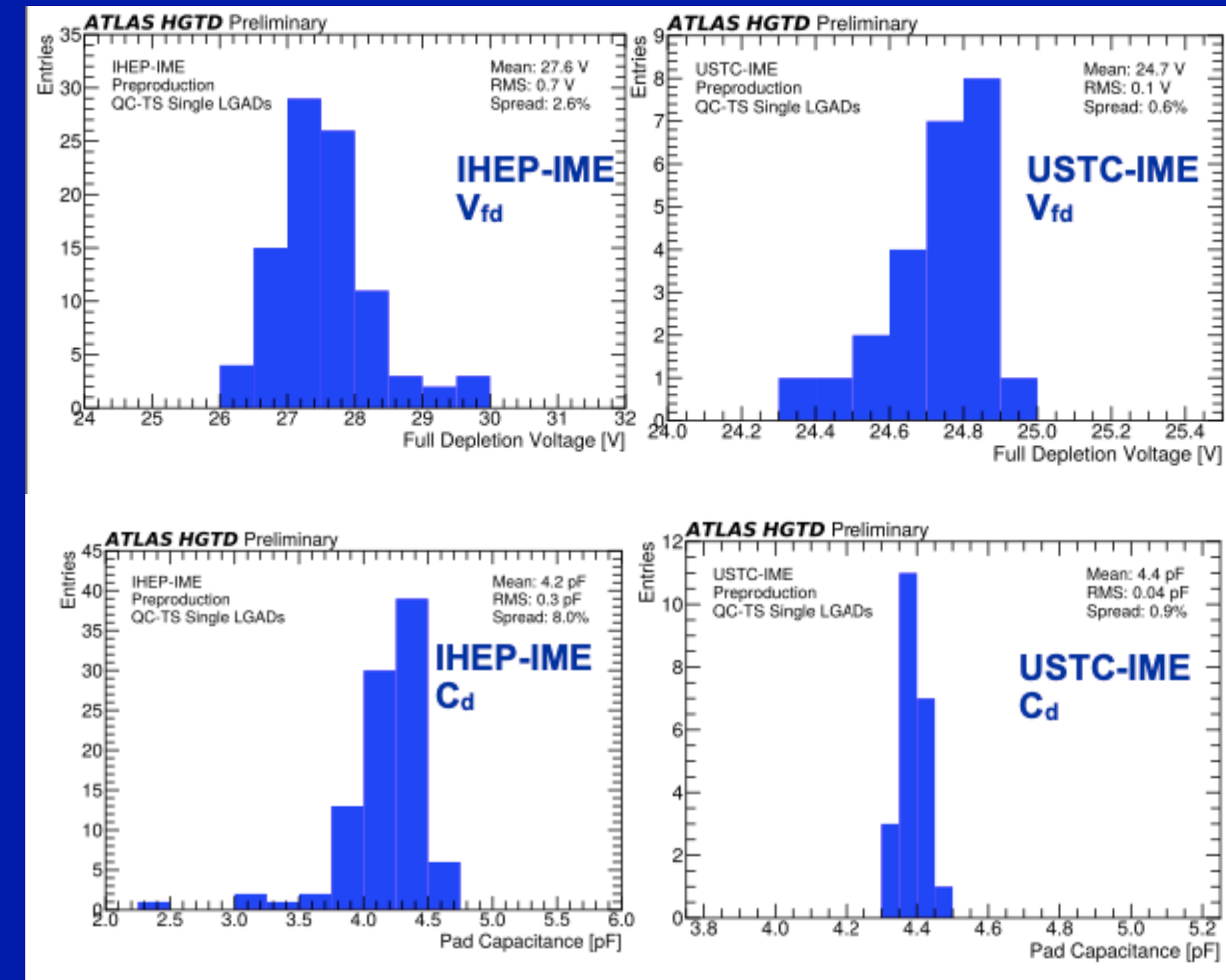
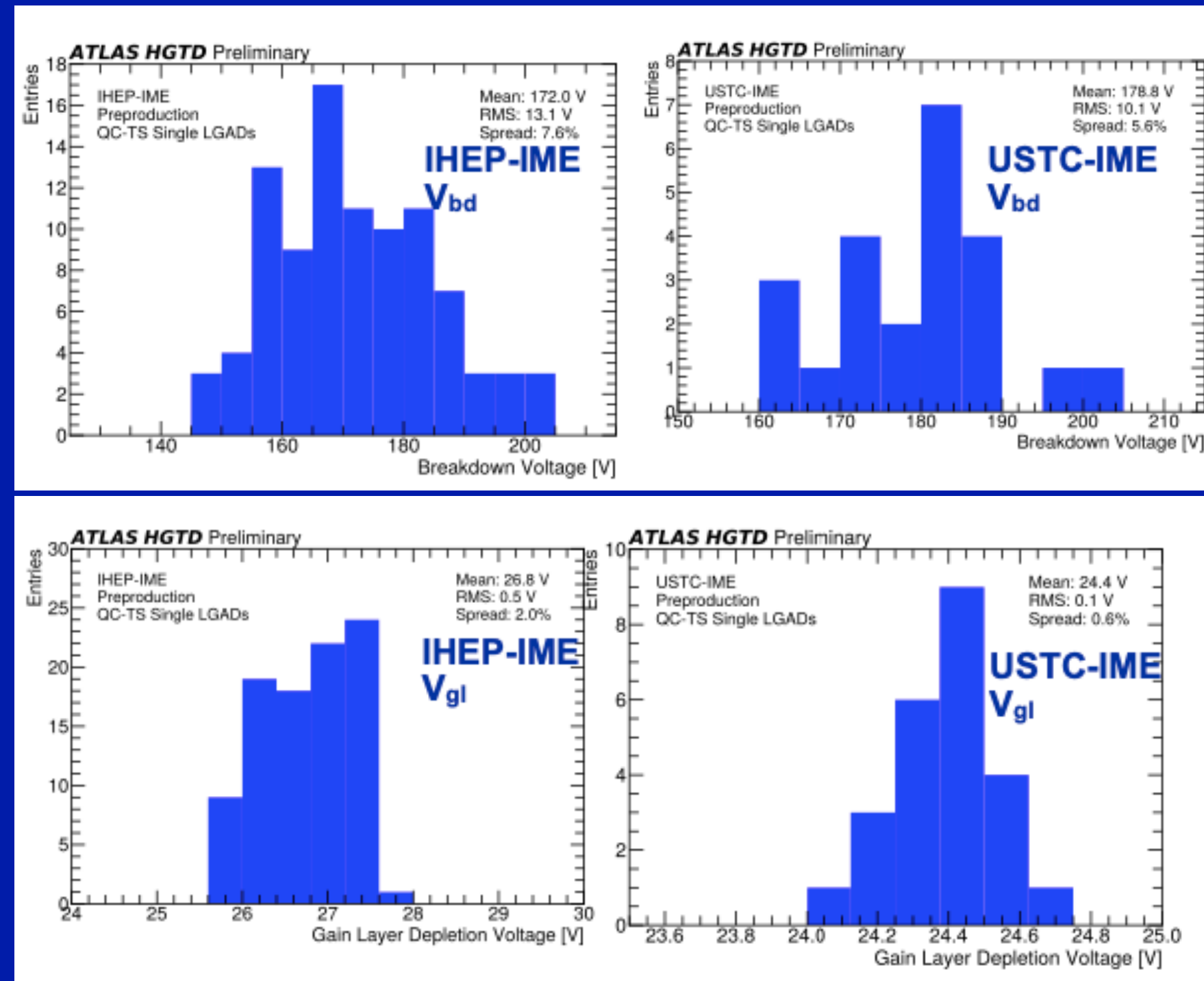
- Several fluences studied:  $^{90}\text{Sr}$  data for fluences of  $2.5 \times 10^{15} \text{ n}_{eq} \text{ cm}^{-2}$  and above are shown for the operating voltage at the SEB limit of 550 V
- Data for each design is fitted with a linear fit and uncertainty band represents  $1\sigma$  fit parameter variation
- The wafer acceptance threshold is defined by the point where the fit intersects a charge of 5 fC

Measurements on ~10 QC-TS per wafer for IHEP-IME and USTC-IME

<https://indico.cern.ch/event/1386009/contributions/6279120>

## Gain layer properties

## Substrate properties



Breakdown of single-pad sensor defined as: V @ 500 nA

- $V_{bd}$  spread:  
7.59% for IHEP-IME and 5.64% for USTC-IME → within specs (8%)

Gain layer depletion voltage:

- Specification:  $24V < V_{gl} < 55V$  with spread 2.02% for IHEP-IME and 0.57% for USTC-IME

All wafers met the criteria

Full-depletion voltage [ $V_{fd}$ ]:

- Specification  $< 70 V$  → Spread inside specs ( $< 10\%$ ) for both designs
- Resistivity of the substrate is larger than  $1k\Omega \cdot cm$

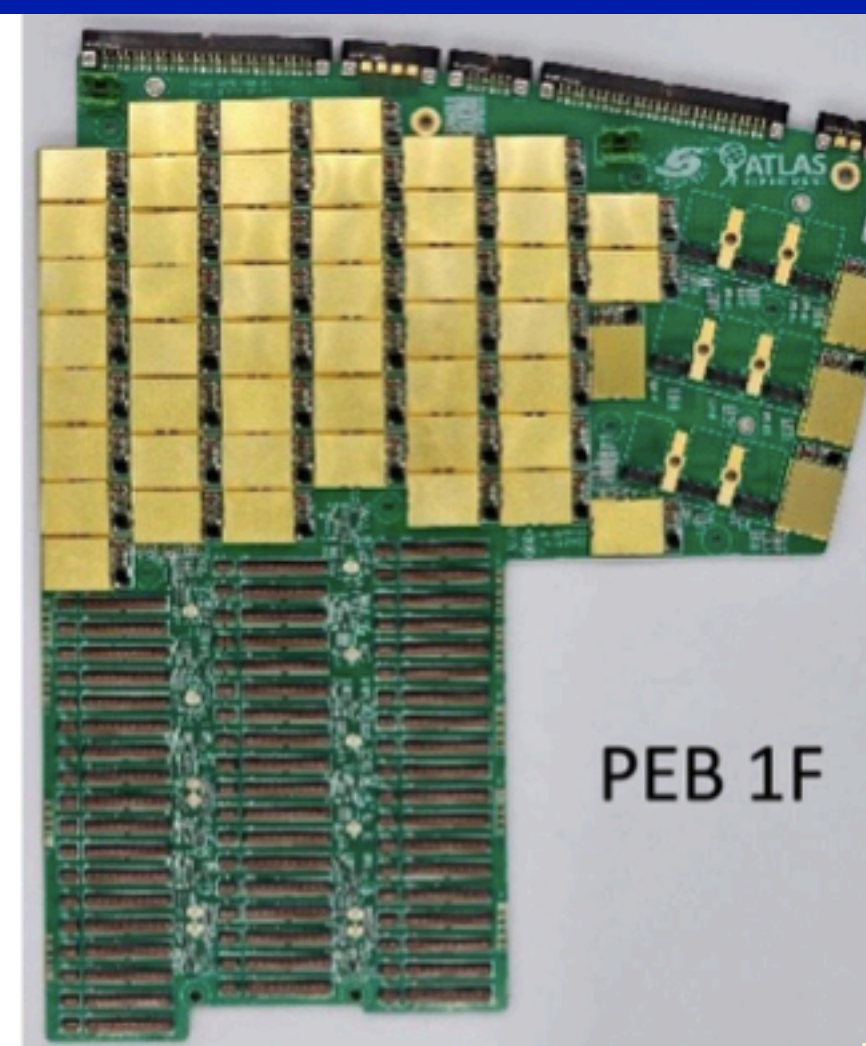
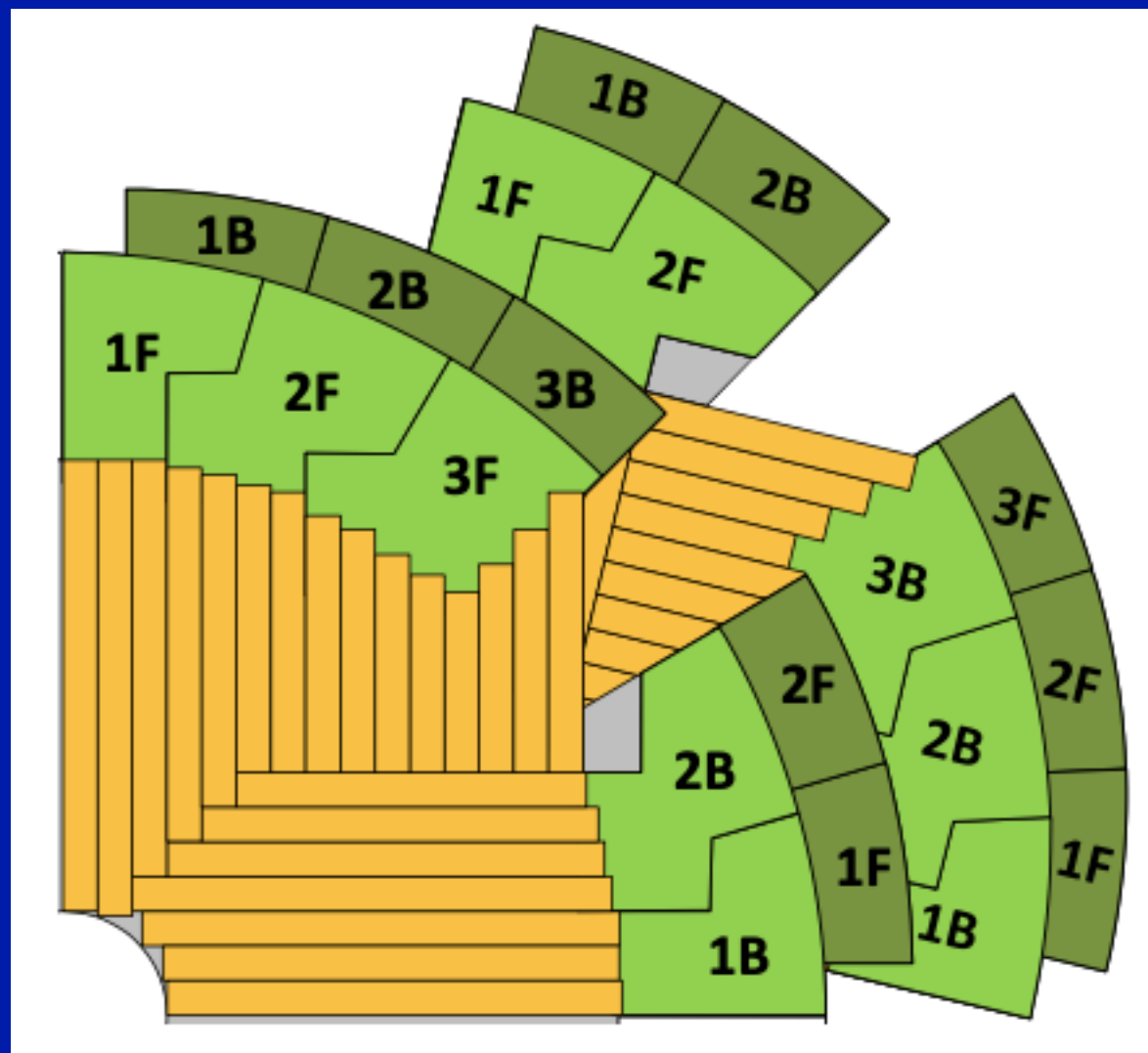
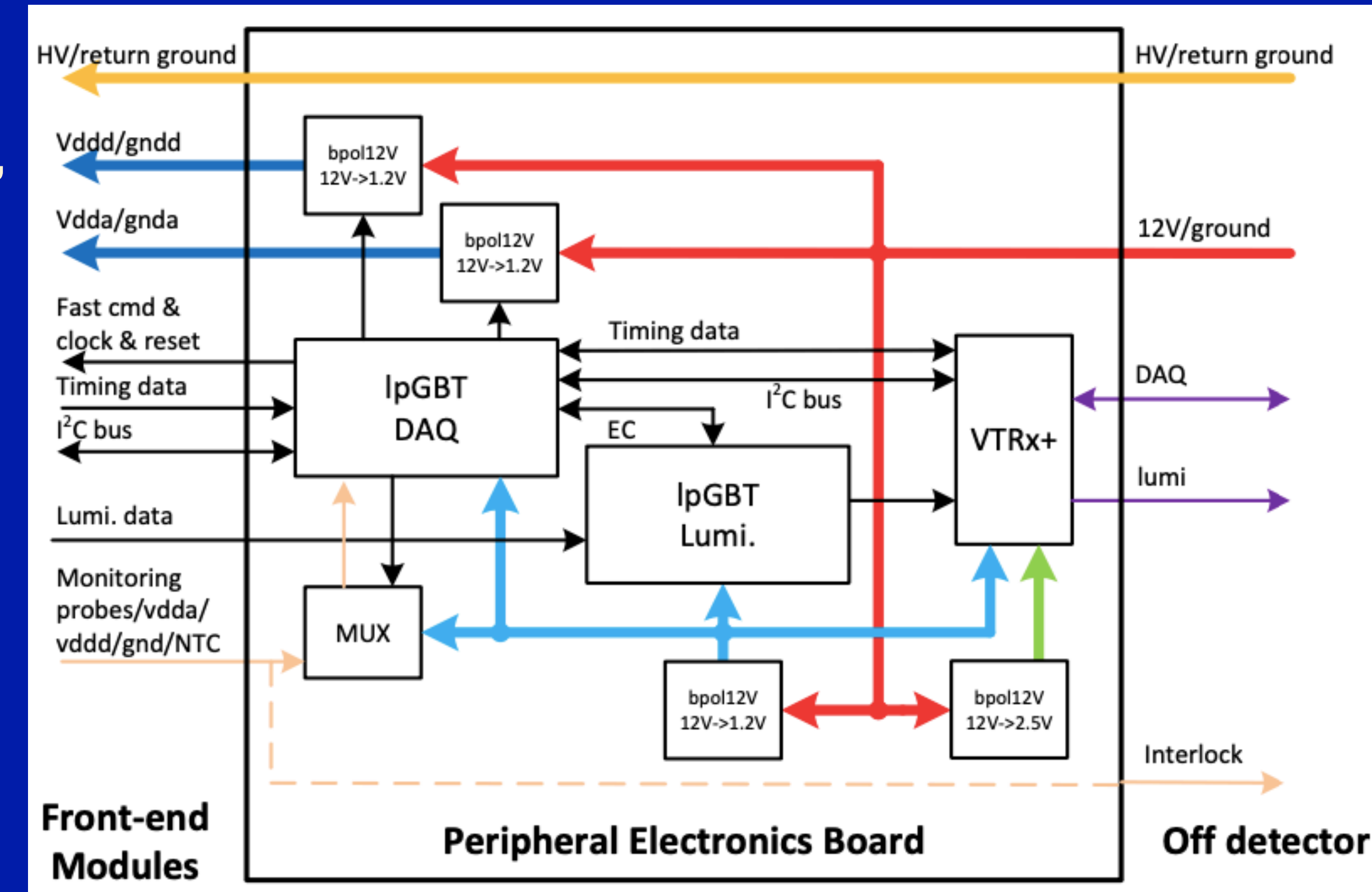
Detector Capacitance [ $C_d$ ]:

- Specs:  $< 4.5 pF$  → met

Results consistent within the specifications / expectations



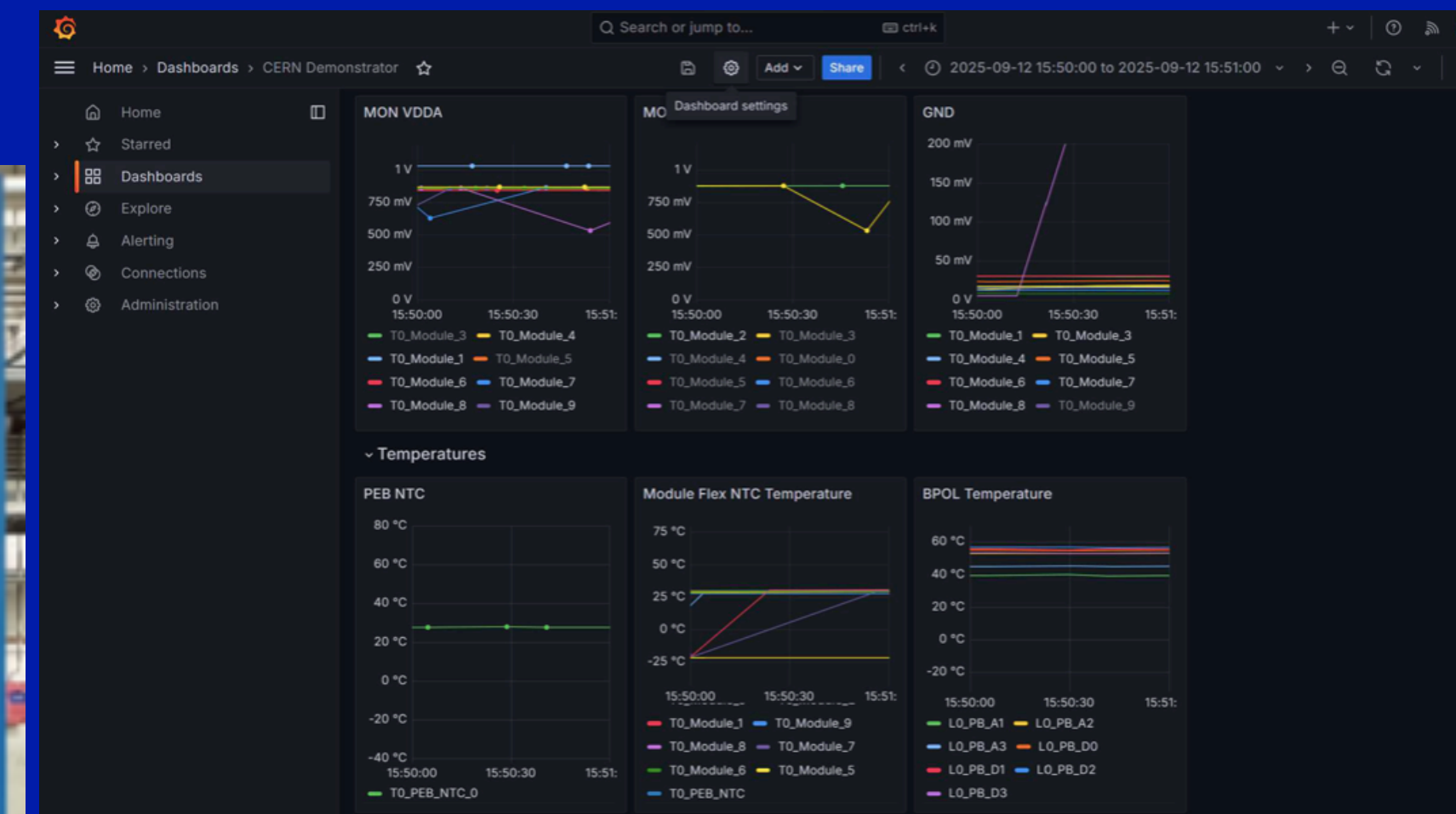
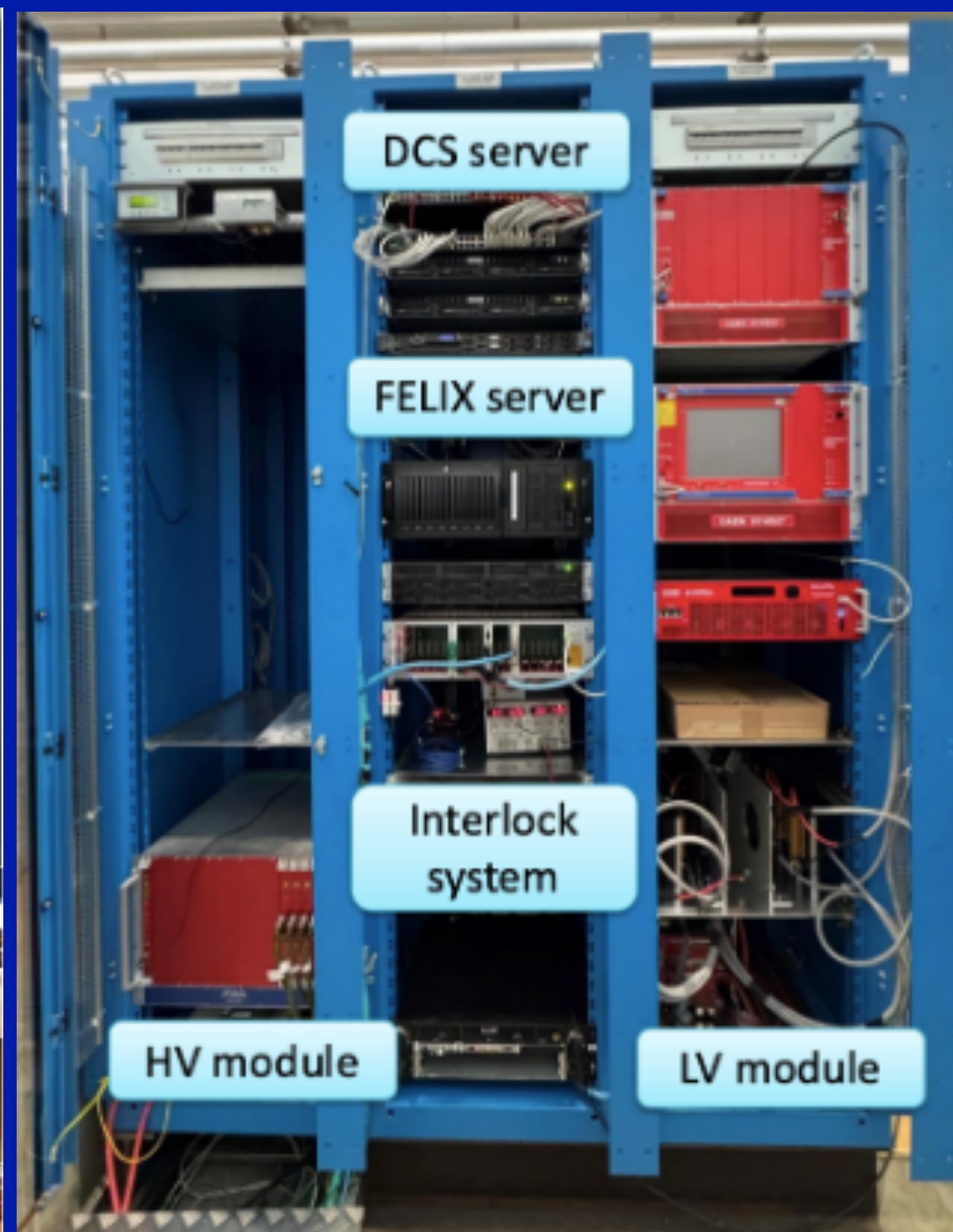
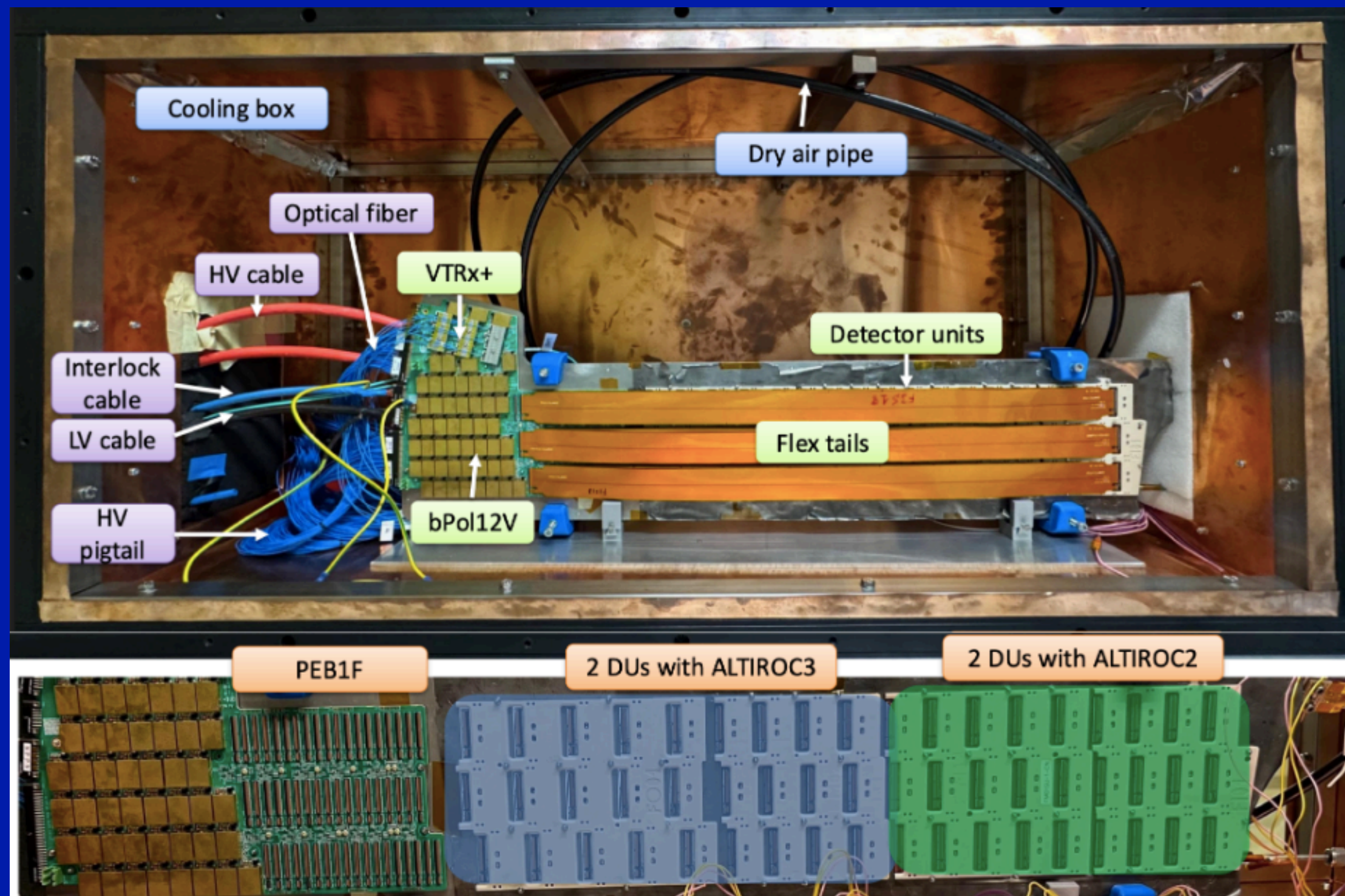
- Handles data transmission, LV & HV, monitoring and control
- Main components: IpGBT (data aggregation), VTRx+ (optical), bPOL12V (LV converters), MUX64
- Dedicated data paths for timing and luminosity
- The PEB1F case: 55 FPC, 52 bPol12V, 12 IpGBT, 9 VTRx+, 9 MUX64 within 9.7 mm thickness
- 22 layer PCB, with HDI micro via and VIPPO techniques, High speed, low loss multi-layer material for impedance control



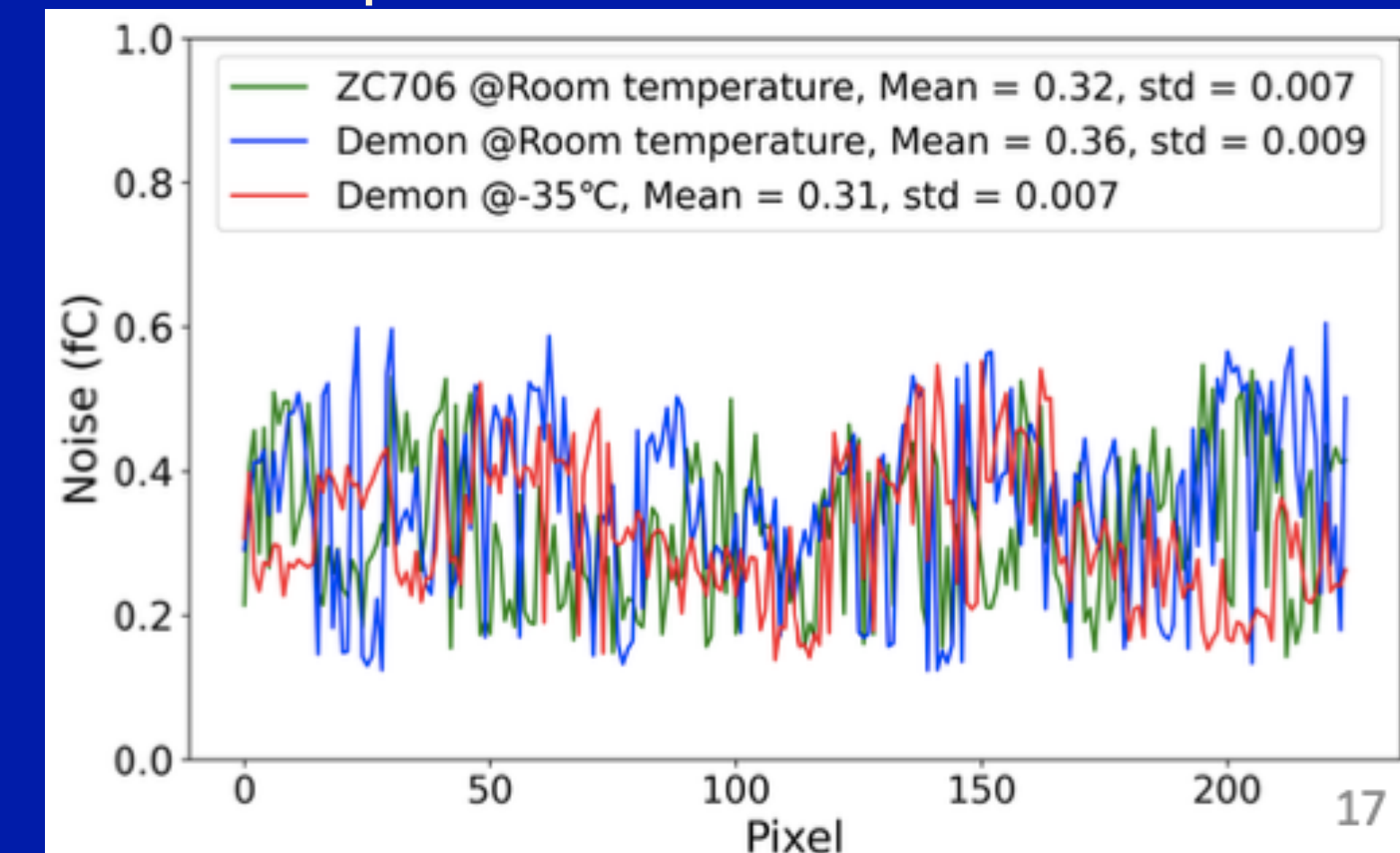
*... the most difficult boards manufactured in HEP projects...,*  
ATLAS P2UG Review committee



- Full chain and detector level test with all components.
- One PEB (1F) connecting 54 modules loaded on 4 support units
- LV + HV + PEB + ALTIROC DUs + cooling + DCS&Interlock in a cold box ( = -30 C)
- Allows system-level testing of all components



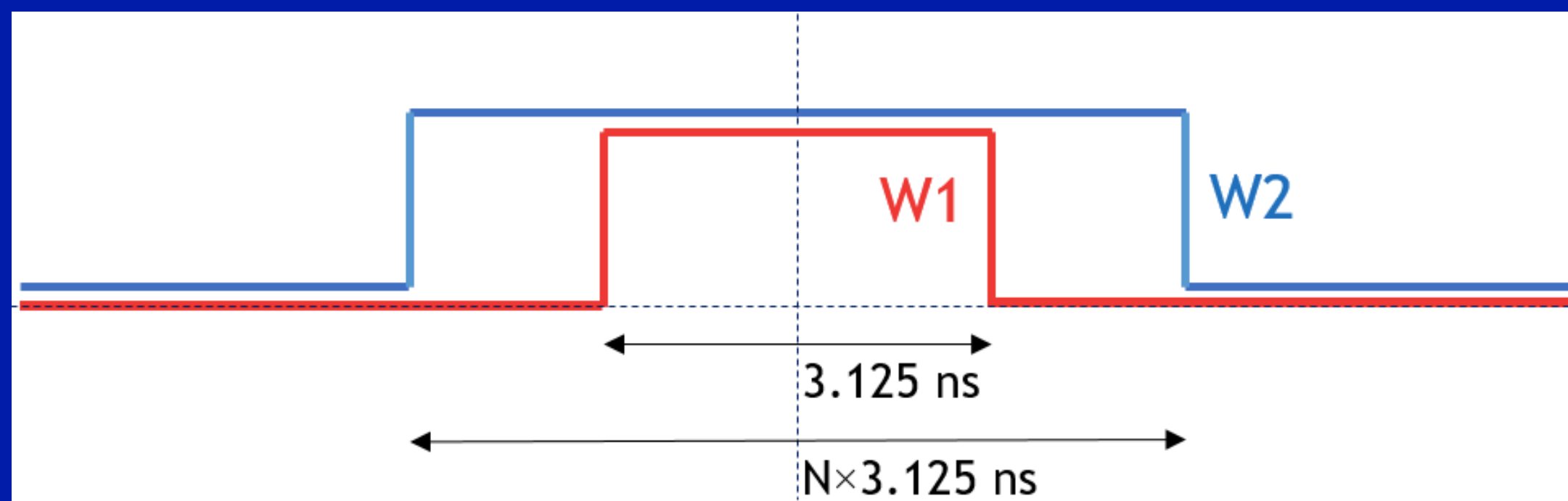
Noise comparison demonstrator/test bench



A Module-0 construction (fully integrated prototype consisting in 1/4 disk) will follow in 2026

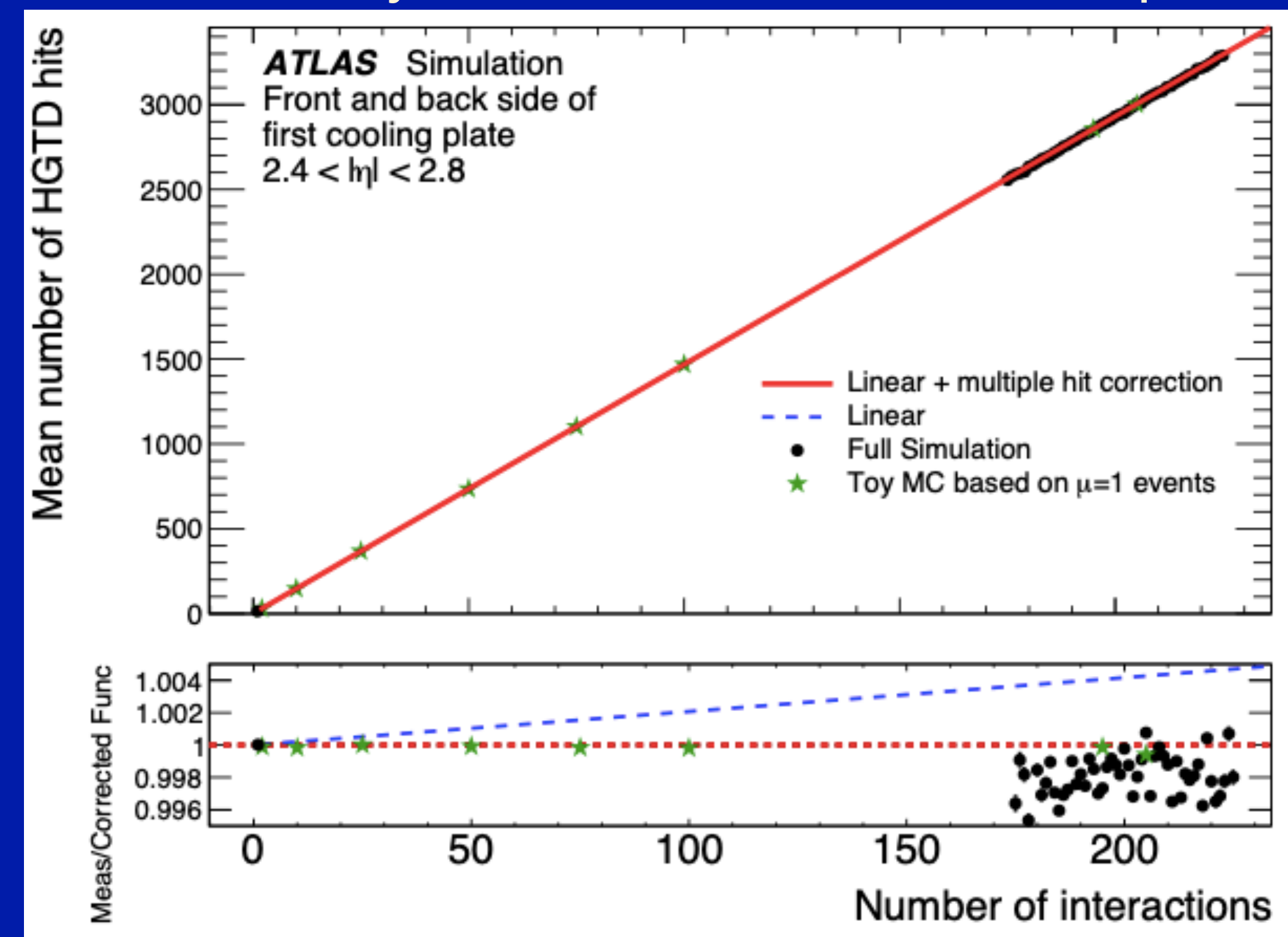


- The high granularity of HGTD ensures an occupancy less than 10%  
→ excellent linearity between the average number of hits and  $\langle\mu\rangle$  over the full range of luminosity expected at the HL-LHC
- ALTIROC in  $2.4 < |\eta| < 2.8$  (outer ring) provides per-sensor occupancy per bunch-crossing with 1% accuracy
- Hit counting at 40 MHz
- Dedicated readout chain, independent of the trigger and timing data



Windows of counting hits centred at the bunch-crossing time  
W2 for background correction

Linearity of  $\langle n_{\text{hits}} \rangle$  as a function of  $\langle\mu\rangle$



**Per-track timing resolution:** 30–50 ps in the forward region, meeting HGTD design targets for precise time tagging of tracks.

**It will allow:**

- strong suppression of pileup tracks and jets, improving event reconstruction in high-luminosity conditions.
- independent bunch-by-bunch luminosity measurement within 1 % precision.

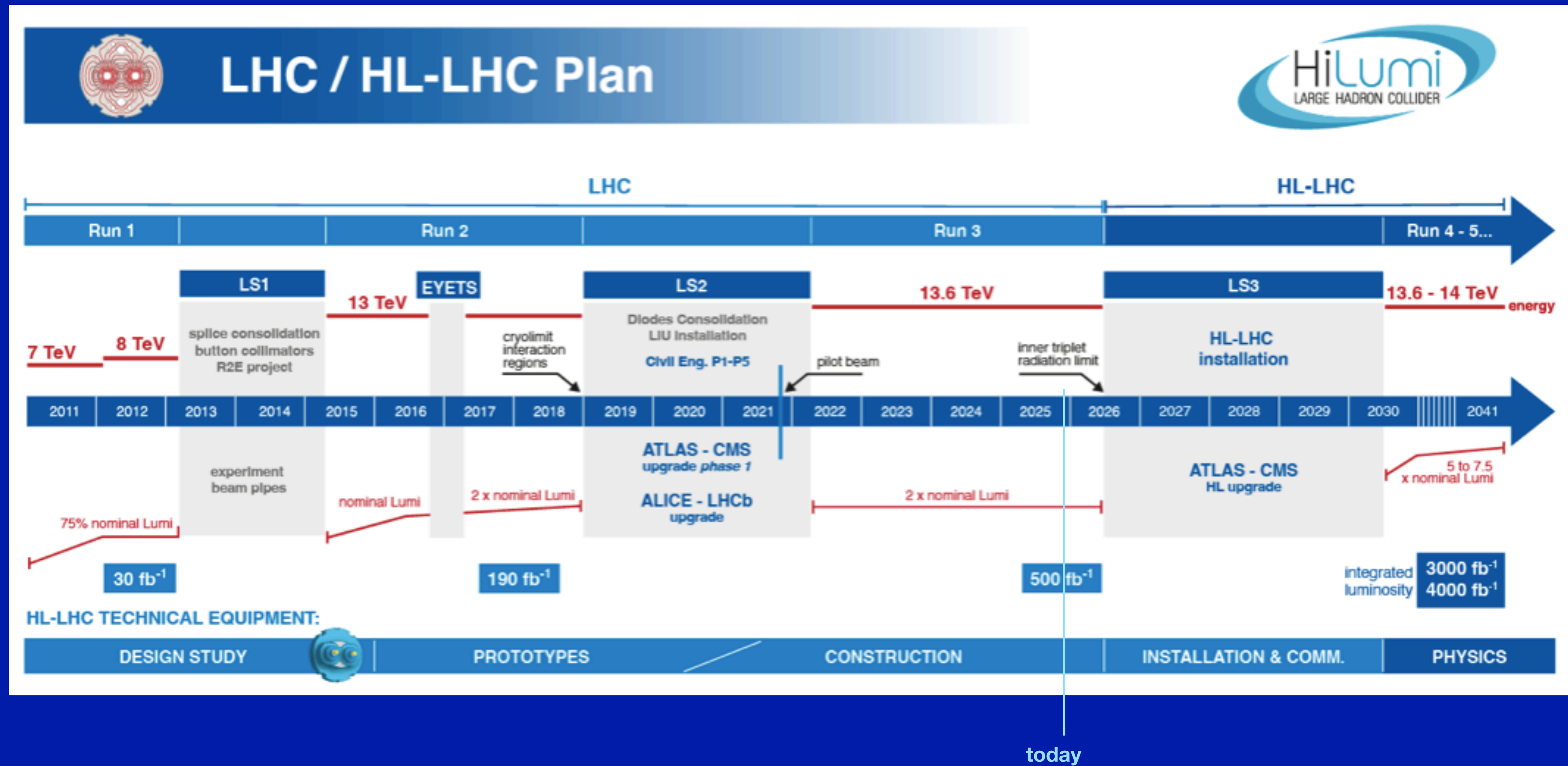
**Project status:**

- The HGTD is transitioning from R&D to production, with several critical components already under QA/QC.
- A busy construction and integration is ongoing, as we move toward Module0 and full detector assembly and installation.

*.....Exciting times ahead!*









## Trigger and Data Acquisition:

- First level trigger at 1 MHz, 5.2 TB/s, 10  $\mu$ s latency
- Event Filter 10 kHz, ~52 GB/s

## Electronics upgrade:

- On/Off-detector electronics for Calorimeters and Muon systems
- 40 MHz readout and finer trigger segmentation

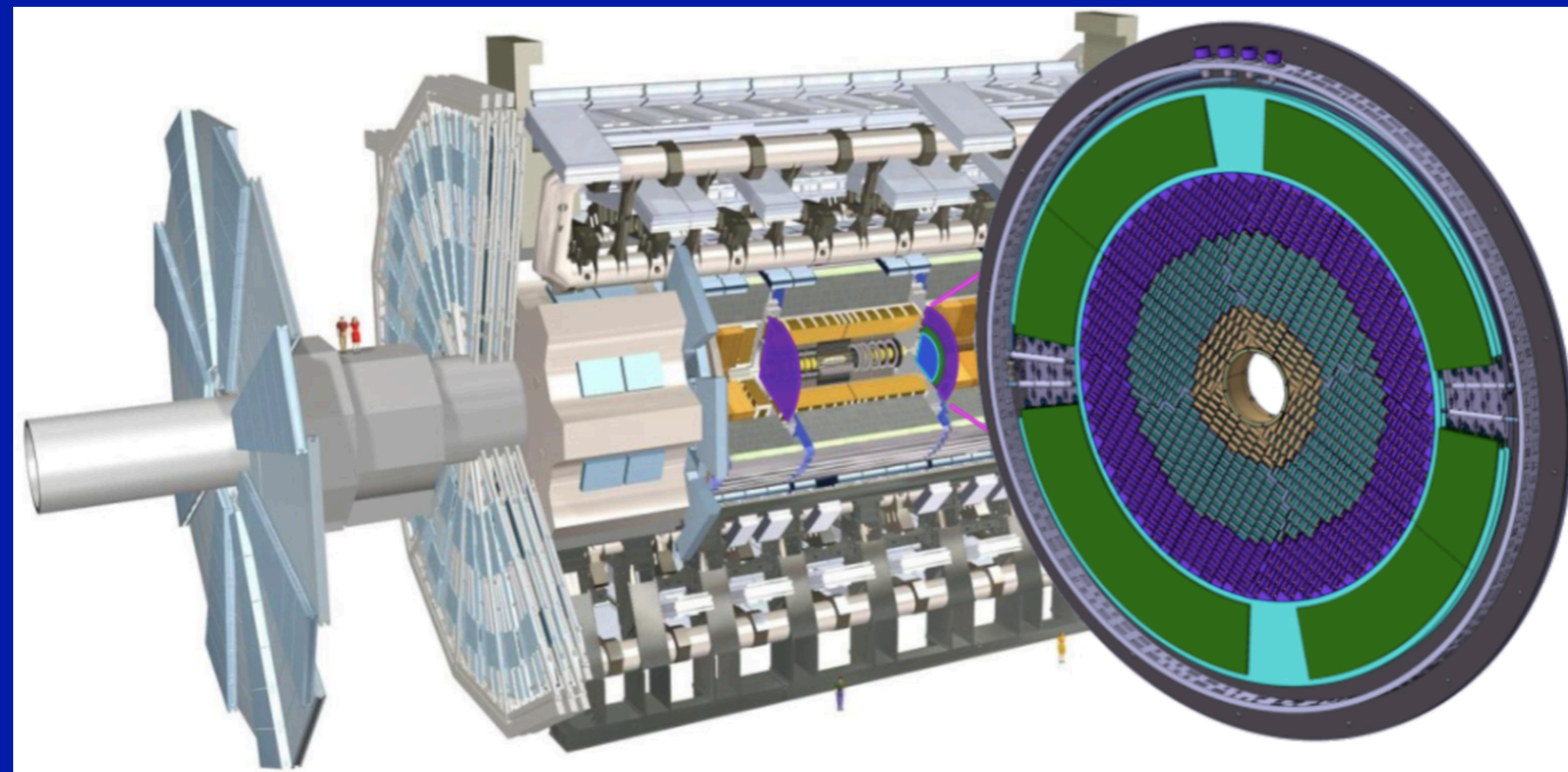
## New Inner Tracker Detector:

- All Silicon
- 9 layers for  $|\eta| < 4$
- Reduced material budget
- Finer segmentation

*T. Koffas' talk*

## New muons chambers:

- Inner barrel with new RPCs, sMDTs and TGCs
- Improves momentum resolution, trigger efficiency and fake rejection

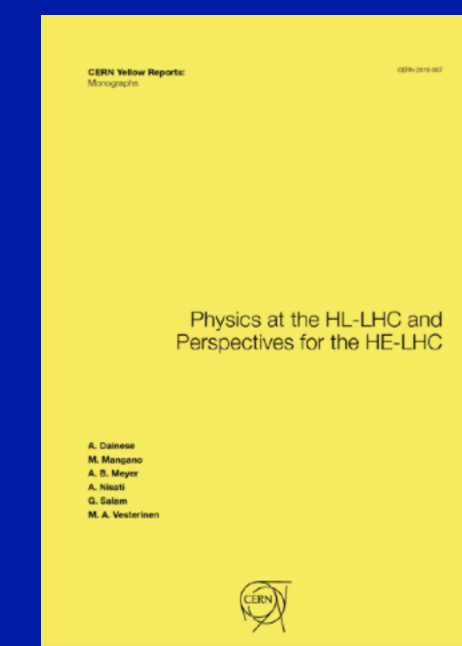


## High Granularity Timing Detector (HGTD):

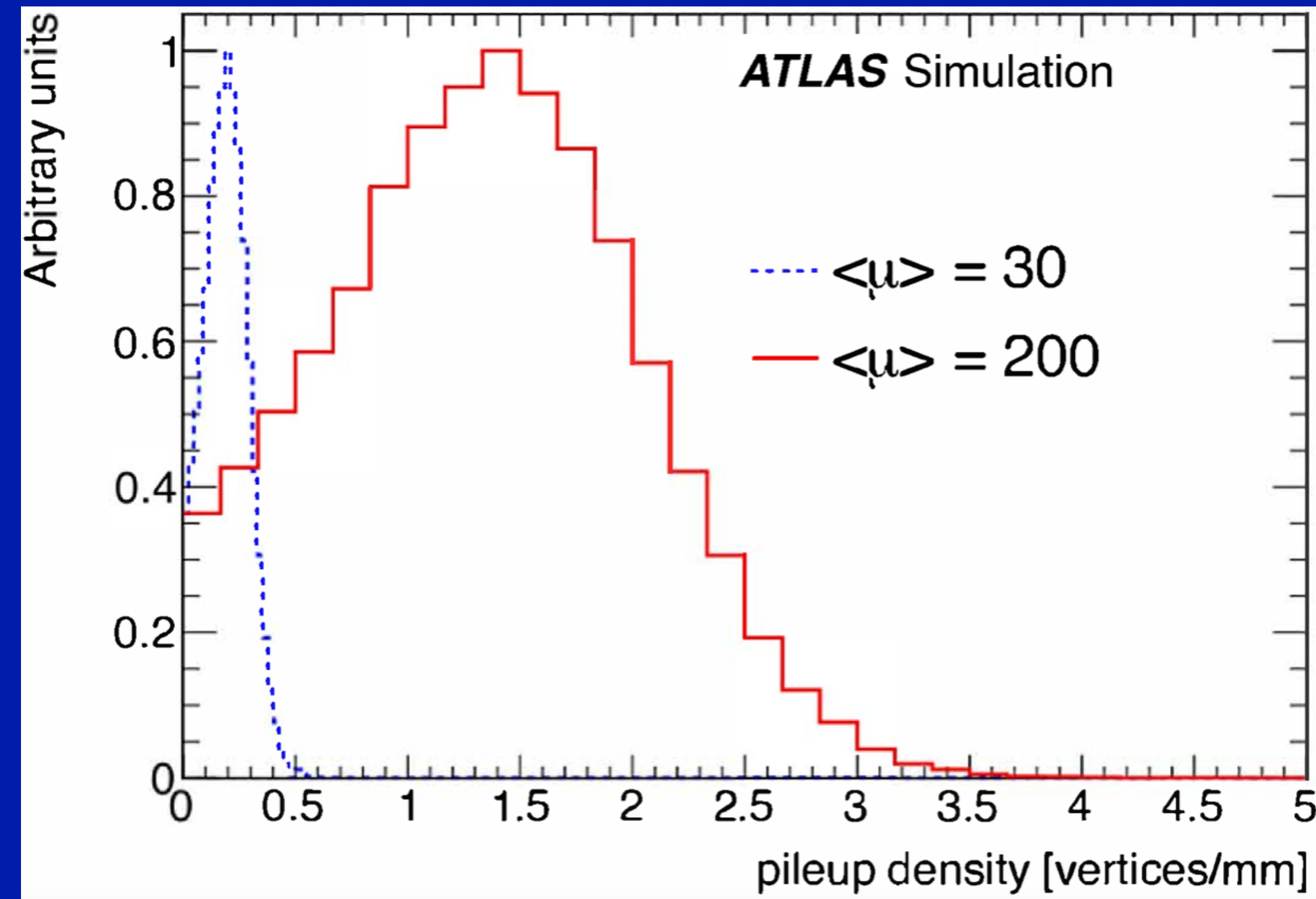
- Precision timing using Silicon Low Gain Avalanche Detectors (LGAD)
- Improves pileup separation and measures luminosity

## Additional upgrades:

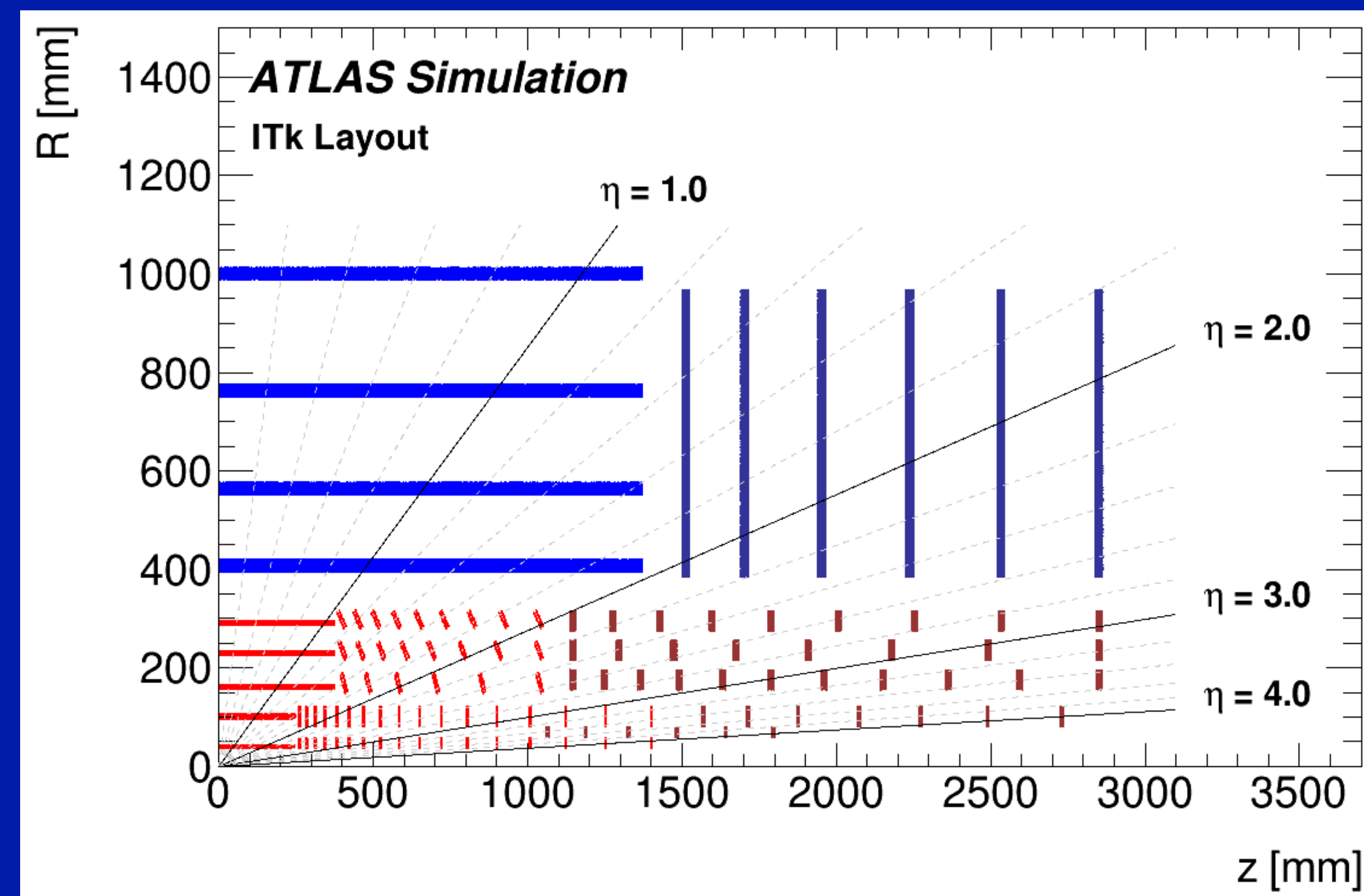
- Luminosity detectors (1% precision),
- Zero degree calorimeter for Heavy Ion physics





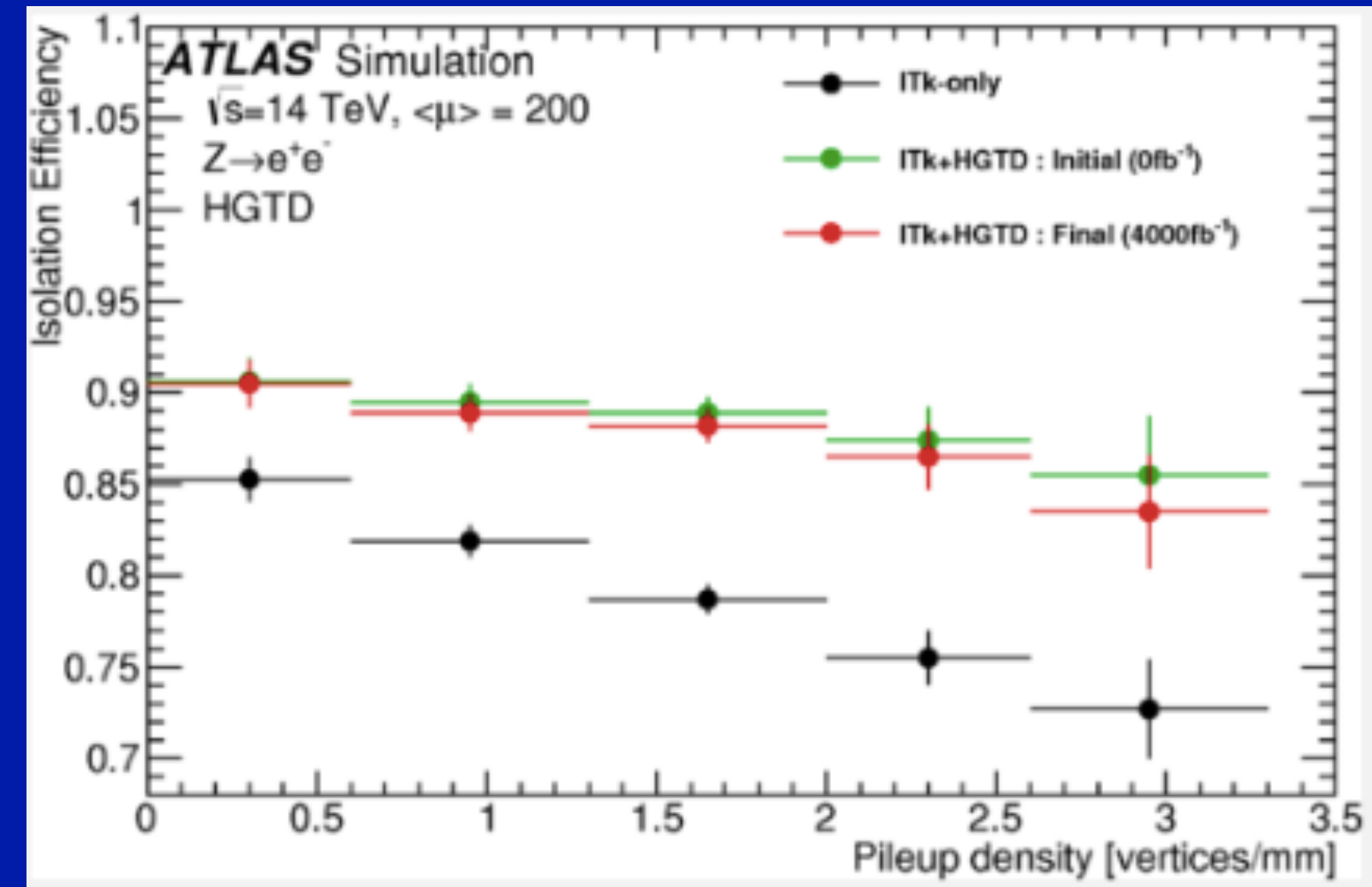
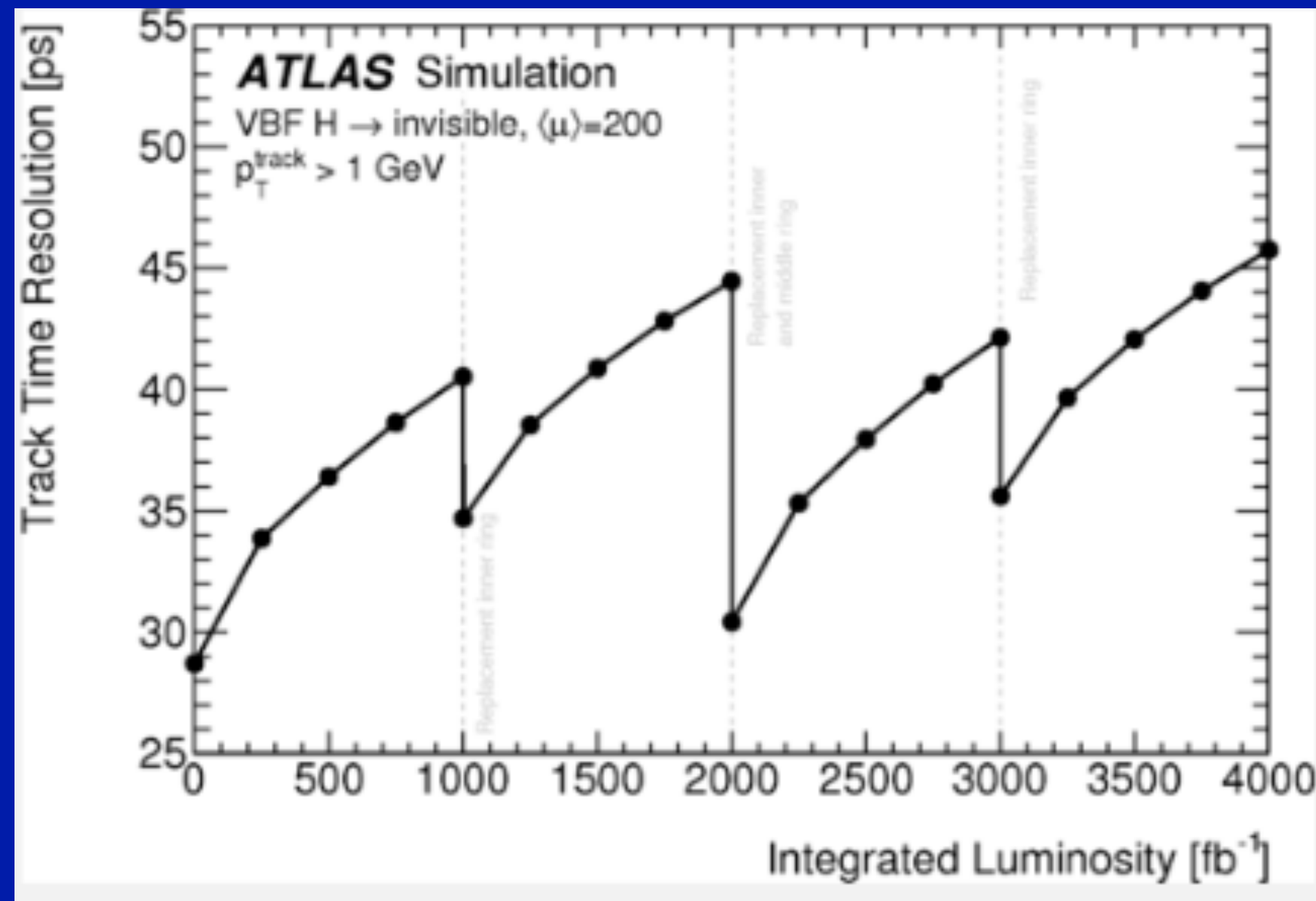


Vertex density in the z-axis

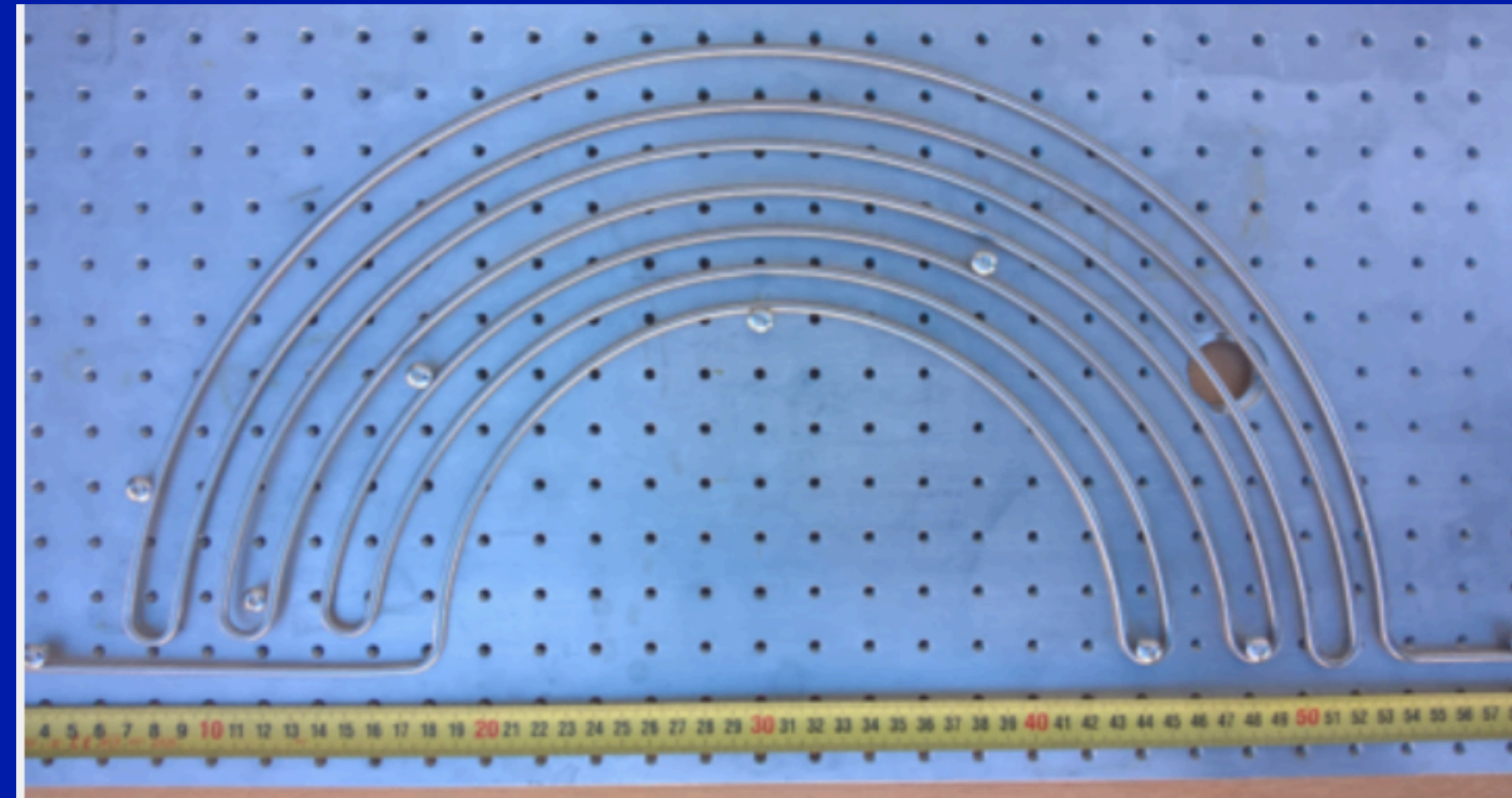
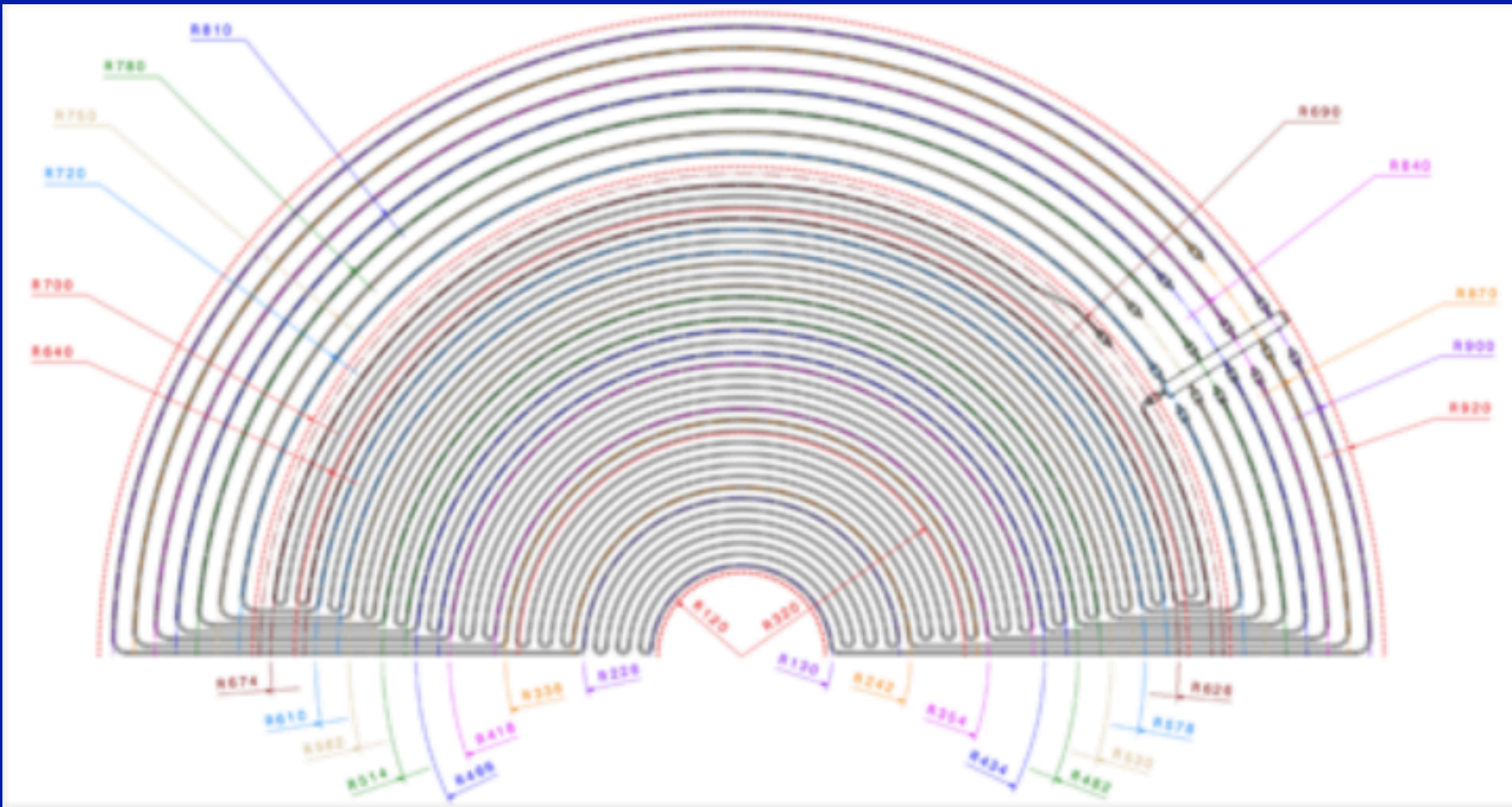


The active elements of the barrel and end-cap ITk Strip detector are shown in blue, for the ITk Pixel detector the sensors are shown in red for the barrel layers and in dark red for the end-cap rings.





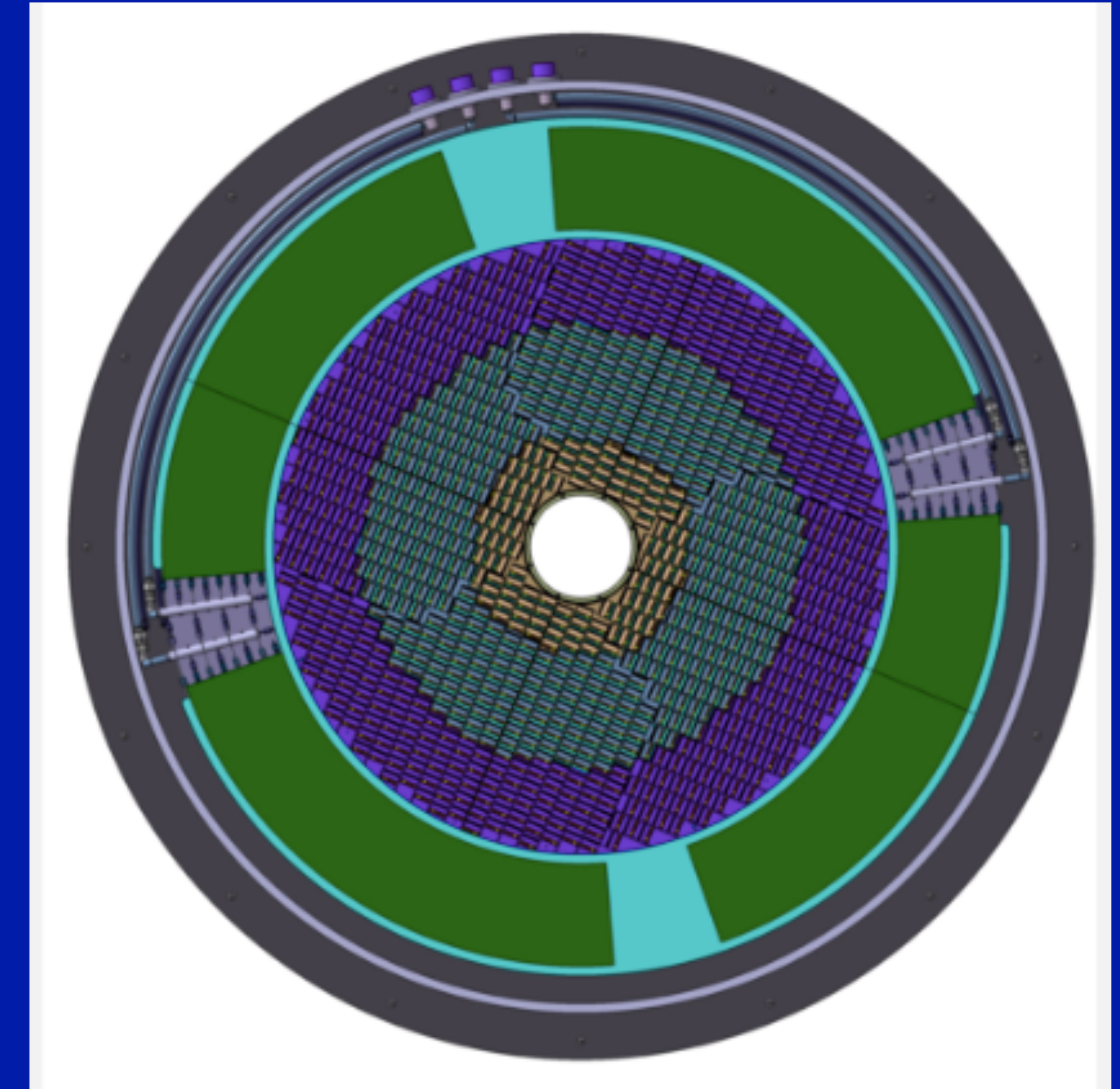
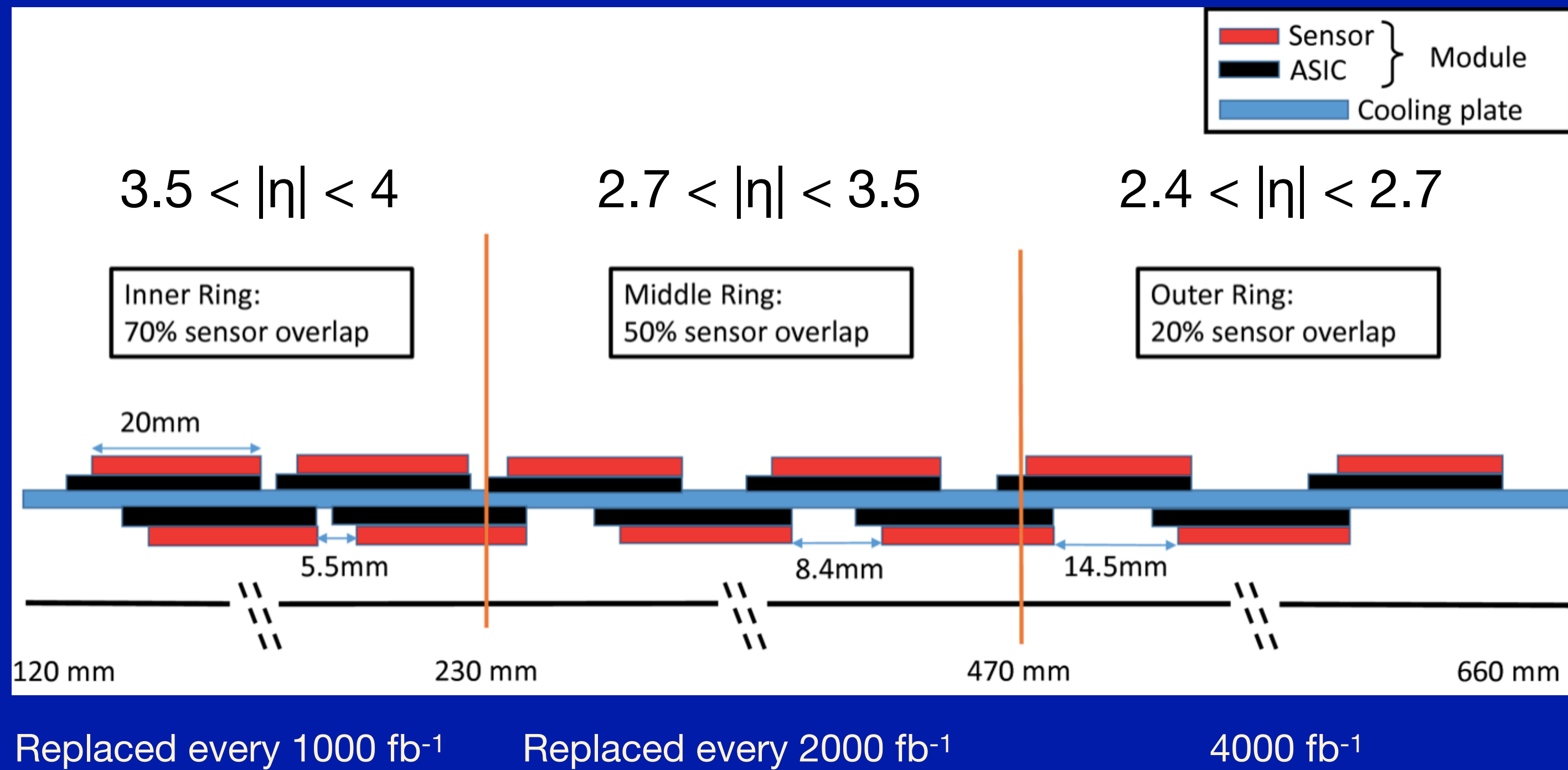






# overlap between the modules on the front and back disks<sup>27</sup>

[HGTD TDR Public Plots](#)



Monitored process parameters during the production

QC Device	Parameter	Description	Technique used
Single LGAD	V <sub>gl</sub>	Gain layer depletion voltage	C-V
	V <sub>fd</sub>	Full depletion voltage of the device	C-V
	I@V <sub>fd</sub>	Current at full depletion voltage	I-V
	V <sub>bd</sub>	Device breakdown voltage	I-V
	C <sub>pad</sub>	Electrode capacitance	C-V
PIN	V <sub>bd</sub>	Breakdown Voltage	I-V
	I <sub>leak</sub>	Leakage Current	I-V
MOS	t <sub>ox</sub>	Oxide Thickness	C-V
	V <sub>fb</sub>	Flatband Voltage	C-V
VDP NA	R <sub>sheet</sub>	Sheet Resistance for N implantation	I-R
VDP PS	R <sub>sheet</sub>	Sheet Resistance for P implantation	I-R
VDP Al	R <sub>sheet</sub>	Sheet Resistance for Aluminum	I-R